Modulation of TRPM2 by acidic pH and the underlying mechanisms for pH sensitivity

Jianyang Du, Jia Xie, and Lixia Yue

Department of Cell Biology, Center for Cardiology and Cardiovascular Biology, University of Connecticut Health Center, Farmington, CT 06030

TRPM2 is a Ca^{2+}-permeable nonselective cation channel that plays important roles in oxidative stress–mediated cell death and inflammation processes. However, how TRPM2 is regulated under physiological and pathological conditions is not fully understood. Here, we report that both intracellular and extracellular protons block TRPM2 by inhibiting channel gating. We demonstrate that external protons block TRPM2 with an IC_{50} of pH_o = 5.3, whereas internal protons inhibit TRPM2 with an IC_{50} of pH_i = 6.7. Extracellular protons inhibit TRPM2 by decreasing single-channel conductance. We identify three titratable residues, H958, D964, and E994, at the outer vestibule of the channel pore that are responsible for pH_o sensitivity. Mutations of these residues reduce single-channel conductance, decrease external Ca^{2+} ($[Ca^{2+}]_o$) affinity, and inhibit $[Ca^{2+}]_o$-mediated TRPM2 gating. These results support the following model: titration of H958, D964, and E994 by external protons inhibits TRPM2 gating by causing conformation change of the channel, and/or by decreasing local Ca^{2+} concentration at the outer vestibule, therefore reducing $[Ca^{2+}]_o$ permeation and inhibiting $[Ca^{2+}]_o$-mediated TRPM2 gating. We find that intracellular protons inhibit TRPM2 by inducing channel closure without changing channel conductance. We identify that D933 located at the C terminus of the S4-S5 linker is responsible for intracellular pH sensitivity. Replacement of Asp^{933} by Asn^{933} changes the IC_{50} from pH_i = 6.7 to pH_i = 5.5. Moreover, substitution of Asp^{933} with various residues produces marked changes in proton sensitivity, intracellular ADP ribose/Ca^{2+} sensitivity, and gating profiles of TRPM2. These results indicate that D933 is not only essential for intracellular pH sensitivity, but it is also crucial for TRPM2 channel gating. Collectively, our findings provide a novel mechanism for TRPM2 modulation as well as molecular determinants for pH regulation of TRPM2. Inhibition of TRPM2 by acidic pH may represent an endogenous mechanism governing TRPM2 gating and its physiological/pathological functions.

INTRODUCTION

Transient receptor potential (TRP) channels are considered intrinsic sensors of the cellular environment (Clapham, 2003). They are able to sense temperature, voltage, osmolarity, ionic homeostasis, proton concentrations, and a variety of intracellular signaling pathways (Clapham, 2003; Nilius, 2007; Venkatachalam and Montell, 2007). Sensitivity to various chemical, physical, physiological, and pathological stimuli has become a hallmark of TRP channels and also confers their diverse physiological and pathological functions.

TRPM2, also referred to as TRPC7 (Nagamine et al., 1998) or LTRPC2 (Perraud et al., 2001; Sano et al., 2001; Hara et al., 2002), is a member of the melastatin-related TRP (TRPM) channel subfamily (Clapham, 2003; Montell, 2005), which possesses both ion channel and ADP ribose (ADPR) hydrolase functions (Perraud et al., 2001; Sano et al., 2001; Hara et al., 2002). TRPM2 is expressed in various regions of the brain (Nagamine et al., 1998; Perraud et al., 2001; Hara et al., 2002) and in other tissues, including the spleen, heart, liver, lung, and bone marrow (Nagamine et al., 1998; Perraud et al., 2001; Hara et al., 2002). Endogenous TRPM2 currents have been reported in neuronal cells (Hill et al., 2006) and a variety of other types of cells (Herson et al., 1997; Herson and Ashford, 1997; Heiner et al., 2003b, 2005; Kraft et al., 2004; Beck et al., 2006; Carter et al., 2006; Hecquet et al., 2008). TRPM2 is a Ca^{2+}-permeable nonselective cation channel involved in aggravating inflammation (Yamamoto et al., 2008), oxidative stress–mediated cortical and striatal neuronal cell death (Fonfria et al., 2005; Kaneko et al., 2006), hematopoietic cell death (Hara et al., 2002; Kaneko et al., 2006; Zhang et al., 2006), and insulin secretion (Togashi et al., 2006).

TRPM2 can be activated by ADPR (Perraud et al., 2001; Sano et al., 2001), cADPR (Kolisek et al., 2005), oxidative stress (Hara et al., 2002; Wehage et al., 2002; Naziroglu and Luckhoff, 2008), NAD^+ (Sano et al., 2001; Hara et al., 2002; Heiner et al., 2003a), and intracellular Ca^{2+} (Du et al., 2009). ADPR activates TRPM2 by directly binding to the channel's enzymatic NUDT9-H domain

Correspondence to Lixia Yue: lyue@uchc.edu

Abbreviations used in this paper: ADPR, ADP ribose; HP, holding potential; NMDG-Glu, NMDG glutamate; TRP, transient receptor potential; TRPM, melastatin-related TRP; WT, wild-type.

The Rockefeller University Press $30.00
J. Gen. Physiol. Vol. 134 No. 6 471–488
www.jgp.org/cgi/doi/10.1085/jgp.200910254

(Kühn and Lückhoff, 2004; Perraud et al., 2005). Intracellular Ca^{2+} can activate TRPM2 (Du et al., 2009) and also synergize ADPR- and cADPR-mediated TRPM2 activation (Perraud et al., 2001; McHugh et al., 2003; Beck et al., 2006). An increase in $[Ca^{2+}]_i$ levels significantly reduces the ADPR concentration required for TRPM2 activation (Perraud et al., 2001). Moreover, ADPR and cADPR can synergistically activate TRPM2 (Kolisek et al., 2005; Beck et al., 2006).

Once activated, TRPM2 channels conduct large inward and outward currents with a linear I-V relation. In the heterologous expression system, TRPM2 activated by ADPR/Ca^{2+} can be as large as 10–20 nA (Perraud et al., 2001; Sano et al., 2001; Hara et al., 2002). Endogenous TRPM2 activated by ADPR/Ca^{2+} can readily reach 1 nA. As $[Ca^{2+}]_i$ accelerates ADPR-mediated TRPM2 activation, Ca^{2+} entry through TRPM2 serves as a positive feedback for TRPM2 activation. Moreover, the metabolites generated in the NAD^+ pathway, including ADPR and cADPR, synergize with each other to activate TRPM2 (Kolisek et al., 2005; Beck et al., 2006). Therefore, it seems that activation of TRPM2 will initiate a positive feedback that will lead to maximal activation of the channel and ultimately result in cell death due to Ca^{2+} overload. Interestingly, TRPM2 is also involved in other cellular (Togashi et al., 2006) and physiological (Yamamoto et al., 2008) functions in addition to causing cell death, suggesting that other gating mechanisms or regulatory pathways are involved in governing TRPM2 channel functions.

To gain a better understanding as to how TRPM2 gating is regulated under physiological and/or pathological conditions, we investigated whether intracellular and extracellular acidic pH modulates TRPM2 channel functions. We report here that TRPM2 is inhibited by both intracellular and extracellular acidic pH. Although intracellular protons inhibit TRPM2 by inducing channel closure, extracellular protons block TRPM2 by reducing single-channel conductance. We establish that the external residues H958, D964, and E994 are the molecular determinants for pH_o sensitivity. Mutations of these residues inhibit single-channel conductance and reduce $[Ca^{2+}]_o$ affinity as well as $[Ca^{2+}]_o$-mediated TRPM2 gating. Intracellular protons outcompete $[Ca^{2+}]_i$ and $[ADPR]_i$, thereby leading to inhibition of $[Ca^{2+}]_i/[ADPR]_i$-mediated TRPM2 activation. We identify that D933 at the C terminus of the S4-S5 linker is responsible for intracellular proton sensitivity. Mutations of D933 not only substantially reduce pH_i sensitivity and $[Ca^{2+}]_i/[ADPR]_i$ sensitivity, but also markedly alter TRPM2 gating properties. These results indicate that D933 could be an important residue of the intracellular gate, which can sense intracellular proton concentrations, regulate $[Ca^{2+}]_i/[ADPR]_i$-mediated TRPM2 gating, and may also act as a $[Ca^{2+}]_o$ binding site to modulate $[Ca^{2+}]_o$-mediated TRPM2 gating.

MATERIALS AND METHODS

Molecular biology

The TRPM2 construct was provided by A. Scharenberg (University of Washington, Seattle, WA). Mutations of TRPM2 were generated by site-directed mutagenesis (QuickChange; Agilent Technologies) according to the manufacturer's instructions. The predicted mutations were verified by sequencing analysis.

Cell culture and functional expression of TRPM2 and the mutants

HEK-293 cells were grown in DMEM/F12 medium supplemented with 10% FBS, 100 U/ml penicillin, and 100 mg/ml streptomycin at 37°C in a humidity-controlled incubator with 5% CO_2. Cells were transiently transfected with wild-type (WT) TRPM2 or its mutants. A green fluorescent protein–containing pTracerCMV2 vector was cotransfected with pcDNA4/TO-FLAG-hTRPM2 or its mutants at a 1:10 ratio into HEK-293 cells by Lipofectamine 2000 (Invitrogen). We used 5 µl Lipofectamine 2000 for transfection of the cells in a 35-mm culture dish. The green fluorescent protein–containing pTracerCMV2 vector and pcDNA4/TO-Flag empty vector were cotransfected as mock controls. Successfully transfected cells can be identified by their green fluorescence when illuminated at 480 nm. Electrophysiological recordings were conducted between 24 and 36 h after transfection. All patch clamp experiments were performed at room temperature (20–25°C).

Electrophysiology

Whole cell and single-channel currents were recorded using an Axopatch 200B amplifier. Data were digitized at 10 or 20 kHz and digitally filtered offline at 1 kHz. Patch electrodes were pulled from borosilicate glass and fire-polished to a resistance of ~3 MΩ when filled with internal solutions. Series resistance (R_s) was compensated up to 90% to reduce series resistance errors to <5 mV. Cells in which R_s was >10 MΩ were discarded (Yue et al., 2002).

For whole cell current recording, voltage stimuli lasting 250 ms were delivered at 1-s intervals, with either voltage ramps or voltage steps ranging from −120 to +100 mV. A holding potential of 0 mV was used for most experiments, unless otherwise stated. A fast perfusion system was used to exchange extracellular solutions, with complete solution exchange achieved in ~1–3 s (Jiang et al., 2005). The internal pipette solution for whole cell current recordings contained (in mM): 135 Cs-methanesulfonate ($CsSO_3CH_3$), 8 NaCl, 0.5 $CaCl_2$, 1 EGTA, and 20 HEPES, with pH adjusted to 7.2 with CsOH. Free $[Ca^{2+}]_i$ was buffered to 100 nM by 1 mM EGTA, unless otherwise specified. 200 µM ADPR was included in the pipette solution for most experiments.

The standard extracellular Tyrode's solution for whole cell current recordings contained (in mM): 145 NaCl, 5 KCl, 2 $CaCl_2$, 1 $MgCl_2$, 10 HEPES, and 10 glucose, with pH adjusted to 7.4 with NaOH. Divalent-free solution contained (in mM): 145 NaCl, 20 HEPES, 5 EGTA, 2 EDTA, and 10 glucose, with estimated free $[Ca^{2+}]$ <1 nM and free $[Mg^{2+}]$ ≈10 nM at pH 7.4. MaxChelator was used to calculate free Ca^{2+} and free Mg^{2+} concentrations. Internal or external Ca^{2+} was adjusted to various concentrations based on calculations using MaxChelator software (Jiang et al., 2005). Internal and external acidic pH solutions were prepared as described previously (Jiang et al., 2005). In brief, 20 mM HEPES used in the solutions at pH 7.0 and 7.4 was replaced by 10 mM HEPES and 10 mM Mes for the solutions at pH ≤ 6. The solutions containing 100 µM to 10 mM Ca^{2+} were prepared from normal Tyrode's solution by adding the appropriate concentration of Ca^{2+}, with reductions in Na^+ concentration when necessary to keep the constant osmolarity. External solutions containing 30 mM NH_4Cl were prepared by decreasing Na^+ concentrations in the Tyrode's solution to keep the constant osmolarity. In experiments

designed to diminish outward currents, pipette solutions contained (in mM): 120 NMDG, 108 glutamic acid, 20 HEPES, 0.5 $CaCl_2$, 1 EGTA, 10 CsCl, and 0.2 ADPR, with pH adjusted to 7.2 with NMDG. The NMDG glutamate (NMDG-Glu) solution used as an external solution contained (in mM): 120 NMDG, 108 glutamic acid, 20 HEPES, and 10 glucose, with pH adjusted to 7.2 with NMDG. When pH 4.5 solution was prepared, 20 mM HEPES was replaced by 10 mM HEPES and 10 mM Mes, and the pH was adjusted to 4.5 with glutamic acid. All the chemicals used in electrophysiological experiments were from Sigma-Aldrich.

Single-channel current recordings were conducted under inside-out configuration. The pipette solution contained (in mM): 140 $NaSO_3CH_3$, 8 NaCl, 2 $CaCl_2$, 10 HEPES, and 10 glucose, with pH 7.4 adjusted with NaOH. The bath solution contained (in mM): 140 $NaSO_3CH_3$, 8 NaCl, and 10 HEPES, with pH 7.2 adjusted with NaOH. Various concentrations of Ca^{2+} or ADPR were added to the bath solutions for some experiments as indicated in the text. An isotonic Ca^{2+} solution containing 120 mM $CaCl_2$, 10 mM HEPES, and 10 mM glucose (pH 7.4) was used as the external solution (pipette solution) for the inside-out experiment in Fig. S3.

Data analysis

Pooled data are presented as mean ± SEM. Dose–response curves were fitted by an equation of the form: $E = E_{max}\{1/[1+(EC_{50}/C)^n]\}$, where E is the effect at concentration C, E_{max} is maximal effect, EC_{50} is the concentration for half-maximal effect, and n is the Hill coefficient (Yue et al., 2000). EC_{50} is replaced by IC_{50} if the effect is an inhibitory effect. Statistical comparisons were made using two-way ANOVA and two-tailed t test with Bonferroni correction. $P < 0.05$ indicated statistical significance.

Online supplemental material

Fig. S1 provides concentration-dependent effects of external protons on the mutants at positions H958, D964, and E994. Fig. S2 shows time-dependent activation and inactivation of H958Q, D964N, and E994Q. Fig. S3 demonstrates Ca^{2+} conductance of D964K compared with that of WT TRPM2. Figs. S1–S3 are available at http://www.jgp.org/cgi/content/full/jgp.200910254/DC1.

RESULTS

Extracellular acidic pH inhibits TRPM2 and alters TRPM2 gating properties

We first investigated the effects of low pH_o on TRPM2 expressed in HEK-293 cells. As shown in Fig. 1, acidic pH_o significantly inhibited TRPM2 in a reversible (Fig. 1 A) and concentration-dependent manner (Fig. 1, B and C). At pH_o 4.0, the inhibition could not be reversed. The IC_{50} for inhibition of TRPM2 was 5.3 pH units (Fig. 1 D). To understand how external protons inhibit TRPM2, we recorded single-channel currents and analyzed single-channel conductance and open probability. As shown in Fig. 2, acidic pH_o markedly reduced single-channel conductance from 75.4 pS at pH_o 7.4 to 43.2 pS at pH_o 5.5 (Fig. 2, A–C). The decrease in single-channel conductance is in agreement with the reduction of macroscopic currents. Therefore, it appears that the decrease in single-channel conductance by extracellular protons can account for the blockade effects of the macroscopic TRPM2 currents by pH_o. We did not analyze the NP_o because the number of channels under each patch could be different for the two groups of experiments.

Because TRPM2 activation is influenced by both internal and external Ca^{2+}, we investigated whether external protons inhibit TRPM2 by influencing $[Ca^{2+}]_o$-mediated TRPM2 activation. Whole cell TRPM2 currents were recorded using pipette solutions containing 500 µM ADPR and a minimal $[Ca^{2+}]_i$ concentration (~1 nM) buffered by 10 mM EGTA. As shown in Fig. 3 A, when the external $[Ca^{2+}]_o$ was changed from 2 mM to 200 µM, the

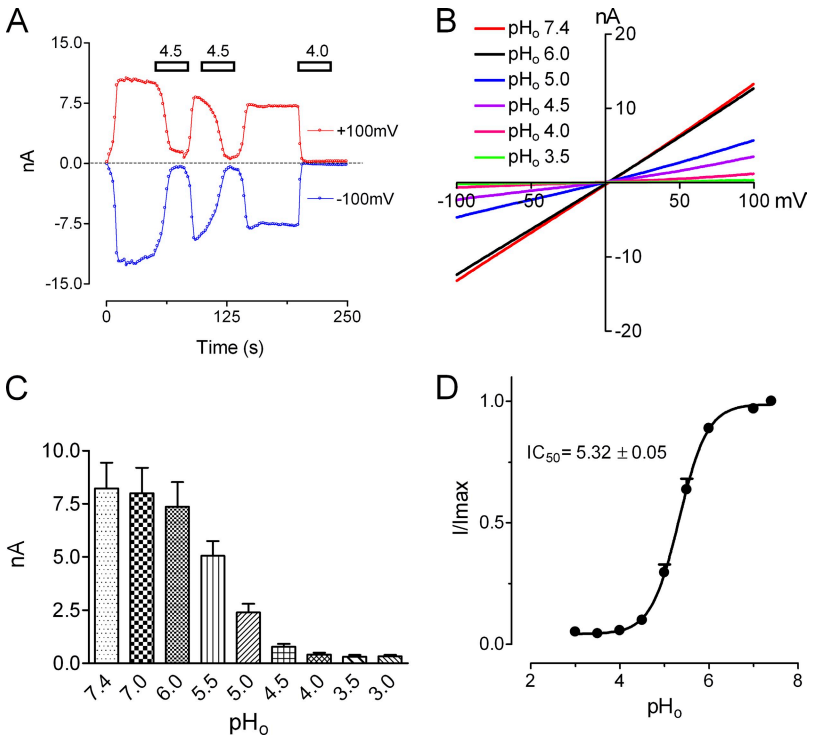

Figure 1. Inhibitory effects of acidic pH_o on TRPM2. (A) Both inward and outward currents of TRPM2 elicited by voltage ramps ranging from −100 to +100 mV were completely and reversibly inhibited by pH_o 4.5. Note that pH_o 4.0 irreversibly blocked TRPM2. Internal pipette solutions contained 100 nM $[Ca^{2+}]_i$ buffered by 1 mM EGTA and 200 µM ADPR. Inward and outward currents were measured at −100 and +100 mV, respectively. (B) Representative recordings of TRPM2 by ramp protocols ranging from −100 to +100 mV at the indicated pH_o. (C) Mean current amplitude of TRPM2 at the indicated pH_o (mean ± SEM; $n = 9$). (D) Dose–response curve of pH_o constructed by normalizing current amplitude at the indicated pH_o to the maximal current amplitude at pH7.4. Best fit of the normalized data yielded an IC_{50} of 5.3 ± 0.05 pH units (mean ± SEM; $n = 9$; Hill coefficient, $n_H = 1.3$).

dose–response curve of external protons was rightward shifted and the IC_{50} was changed from pH_o 5.4 to pH_o 7.5, suggesting that external protons may compete with $[Ca^{2+}]_o$ for binding sites. In contrast to the effects of external Ca^{2+}, changes of internal $[Ca^{2+}]_i$ from 100 nM to 100 μM in the presence of 200 μM $[ADPR]_i$ did not alter the IC_{50}s of external protons on TRPM2, indicating that internal $[Ca^{2+}]_i$ at the range of >100 nM does not influence the effects of external protons on TRPM2. These results also imply that protons may not be able to permeate through TRPM2 channels and exhibit inhibitory effects on TRPM2 from the cytoplasmic side.

TRPM2 is not permeable to protons

To further understand the mechanism by which external protons inhibit TRPM2, we performed a series of experiments to explore whether TRPM2 is permeable to protons that would allow protons to block the channel from the cytoplasmic side. We recorded TRPM2 inward current by holding the cells at −100 mV in the presence of different external solutions. Changing the external solution from NMDG-Cl at pH_o 7.4 to NMDG-Cl at pH_o 4.5 did not produce any inward currents (Fig. 4 A), whereas Tyrode's solution at pH_o 7.4 generated >1,000 pA inward current in the same cell. In mock-transfected control HEK-293 cells, neither NMDG-Cl at pH_o 4.5 nor Tyrode's solution at pH_o 7.4 produced any current (Fig. 4 B). These results suggest that TRPM2 is not permeable to protons. To eliminate influence from other cations, we used NMDG-Glu in the pipette solution and

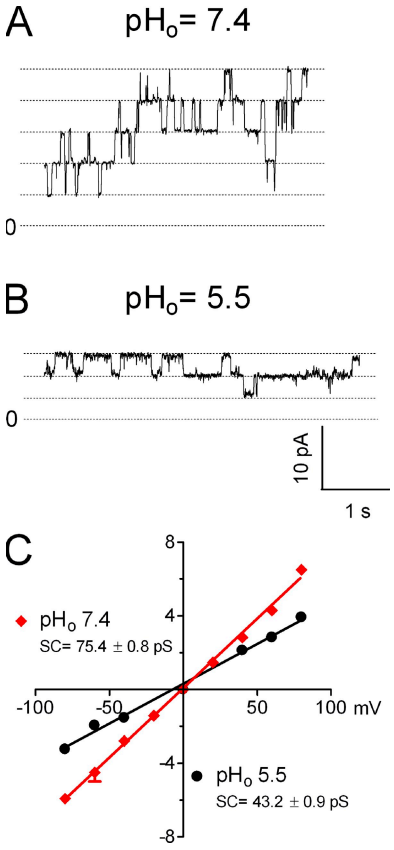

Figure 2. Effects of external protons on single-channel conductance. Single-channel currents were recorded under inside-out configuration with external solutions (pipette solutions) containing 2 mM Ca^{2+} and internal solutions (bath solutions) containing nominal Ca^{2+}-free Tyrode's solution and 200 μM ADPR (pH_o 7.2). (A) Representative recording of TRPM2 at +80 mV with the external solution (pipette solution) at pH_o 7.4. (B) Single-channel recordings of TRPM2 at +80 mV with the external solution (pipette solution) at pH_o 5.5. (C) Average current amplitude at each voltage plotted against the test potential. Linear regression yielded single-channel conductances of 75.4 ± 0.8 pS (mean ± SEM; n = 7∼9) at pH_o 7.4 and 43.2 ± 0.9 pS (mean ± SEM; n = 7∼9) at pH_o 5.5.

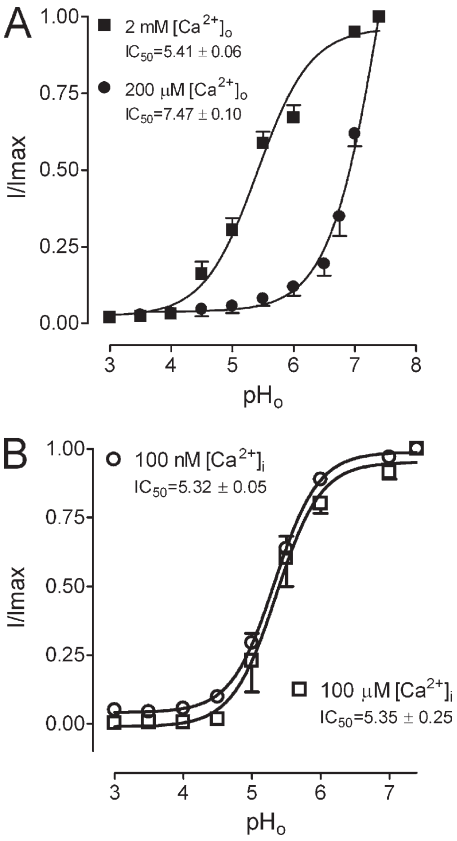

Figure 3. Effects of external and internal Ca^{2+} on protons' inhibition of TRPM2. (A) Concentration-dependent effects of external acidic pH on TRPM2 in the solutions containing 200 μM and 2 mM $[Ca^{2+}]_o$, respectively. Whole cell currents were recorded with pipette solutions containing minimal $[Ca^{2+}]_i$ buffered by 10 mM EGTA and 500 μM ADPR. Ramp protocol (−100 to +100 mV) was used to elicit TRPM2 currents. Current amplitude at +100 mV was measured and normalized to the maximal current amplitude at pH 7.4. The proton dose–response curve was rightward shifted at 200 μM of external $[Ca^{2+}]_o$, and the IC_{50} was changed from 5.4 ± 0.05 pH units (2 mM $[Ca^{2+}]_o$; n = 8) to 7.5 ± 0.1 pH units (200 μM $[Ca^{2+}]_o$; n = 8). (B) Effects of internal $[Ca^{2+}]_i$ on concentration-dependent inhibition of TRPM2 by external protons. Whole cell currents of TRPM2 were recorded in the 2 mM of external Ca^{2+} with pipette solutions containing 100 nM or 100 μM $[Ca^{2+}]_i$ in the presence of 200 μM $[ADPR]_i$. Protons produced similar inhibitory effects on TRPM2 at 100 nM (n = 9) and 100 μM (n = 6) of internal $[Ca^{2+}]_i$ (with 200 μM ADPR), respectively.

used ramp protocol to record TRPM2 currents. Under this condition, TRPM2 produced large inward and small outward currents with a positive reversal potential when the cell was perfused with normal Tyrode's solution. External NMDG-Glu at pH_o 4.5 did not produce any inward current (Fig. 4, C and D). The inward currents measured at −100 mV in various external solutions were plotted as a function of time (Fig. 4 D). No inward proton current was observed in NMDG-Glu at pH_o 4.5 solutions. Mock-transfected cells did not produce any current when perfused with Tyrode's or NMDG-Glu solutions (n = 5). These data further support the notion that protons are not permeant cations.

We further examined concentration-dependent effects of external protons on TRPM2 elicited by ramp protocols by holding the cells at different voltages. The IC_{50} at holding potential (HP) = −100 mV was slightly different from that at HP = 0 mV, but there was no statistical difference (Fig. 4 E). Furthermore, because the blockade effects of pH_o 4.0 on TRPM2 were not reversible, we perfused the cells with external solutions containing 30 mM NH_4Cl to increase pH_i. As shown in Fig. 4 F, 30 mM NH_4Cl was unable to reverse the inhibitory effects of external protons at pH_o 4.0, suggesting that external protons do not permeate through to block TRPM2. Overall, the results summarized in Fig. 4 indicate that TRPM2 is not permeable to external protons.

Molecular mechanisms by which external protons inhibit TRPM2

To investigate the molecular mechanism of extracellular proton inhibition of TRPM2, we created a series of mutations within the extracellular loop between S5 and S6, focusing on amino acid residues that have side chain pKa values in a physiologically relevant range, including His, Glu, and Asp residues (Fig. 5 A). Besides the single mutations, we also generated a triple mutation for the residues H958, E960, and D964 (H958Q-E960Q-D964Q), and a double mutation for the residues of E1010 and D1012 (E1010Q-D1012Q). The resulting TRPM2 mutants were expressed in HEK-293 cells and examined for external proton sensitivity. Except E960Q and the triple mutant H958Q-E960Q-D964N, which resulted in nonfunctional channels, all the other mutants retained channel function with identical linear I-V relation to the WT TRPM2 (Fig. 6). The average

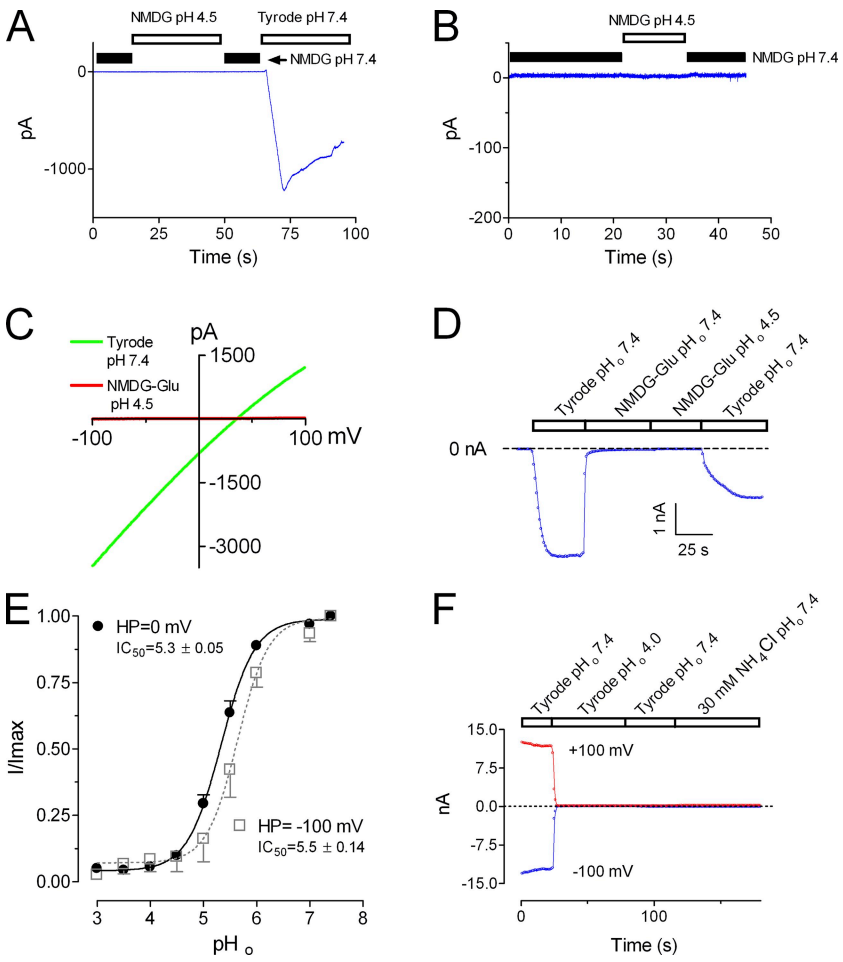

Figure 4. TRPM2 is not permeable to protons. (A) Inward currents of TRPM2 recorded by holding the TRPM2-transfected cell at −100 mV. No current was activated in NMDH-Cl solutions at pH_o 4.5 or 7.4, where Tyrode's solution generated large inward current. (B) In mock-transfected cells, NMDH-Cl solutions at pH_o 4.5 or 7.4 could not induce any current. (C) TRPM2 current elicited by the ramp protocol (−100 to +100 mV) in Tyrode's solution (red). NMDG-Glu at pH_o 4.5 did not induce any inward proton current (green). The pipette solution for this experiment contained NMDG-Glu to favor proton permeation. (D) Inward current of TRPM2 recorded at various external solutions obtained in C. Currents were measured at −100 mV and plotted as a function of time. (E) Effects of holding potentials on the inhibition of TRPM2 by external protons. Dose–response curves were constructed by normalizing the inward currents (−100 mV) at each pH_o to the maximal current amplitude (−100 mV) obtained at pH_o 7.4. The IC_{50}s were 5.3 ± 0.05 (n = 9) at HP = 0 mV and 5.5 ± 0.14 (n = 9; P > 0.05) at HP = −100 mV. (F) Inhibition of TRPM2 by acidic pH_o (pH_o = 4.0) could not be reversed by high pH_i. Inward currents (−100 mV) and outward currents (+100 mV) plotted against time under the indicated conditions. TRPM2 currents were elicited by voltage ramps with the $CsSO_3CH_3$ pipette solution containing 100 nM Ca^{2+} and 200 µM ADPR. Note that TRPM2 was completely and irreversibly blocked by external solutions at pH_o 4.0. 30 mM NH_4Cl, used to increase intracellular pH, could not reverse the effects of pH_o 4. Similar results were obtained in five separate experiments.

current amplitudes of H958Q, D964N, H973Q, E994Q, H995Q, D1002N, E1010Q-D1012N, and E1022Q were indistinguishable from that of WT TRPM2 (Fig. 5 B). However, the mutants at putative selectivity filter, Q981E and D987Q, displayed smaller current amplitude compared with the WT TRPM2 (Fig. 5 B). Although the mutants H973Q, Q981E, D987Q, H995Q, D1002N, E1010Q-D1012N, and E1022Q displayed similar sensitivity to acidic pH_o compared with the WT TRPM2, mutants H958Q, D964N, and E994Q were more sensitive to acidic pH_o (Figs. 5 B and 6). The IC_{50}s were changed from 5.3 for the WT TRPM2 to 6.3, 6.5, and 6.3 pH units for H958Q, D964N, and E994Q, respectively (Fig. 6, G–I).

Because H958Q, D964N, and E994Q are more sensitive to external low pH than the WT TRPM2, we tested whether substitution of H958, D964, and E994 by the residues with different charges and side chains would influence pH_o sensitivity. As shown in Fig. S1, H958A, H958D, and H958K have similar pH sensitivity to that of H958Q. Neutralizing (D964A) or reversing (D964K) the charge at D964 produced graded increases in proton sensitivity. The pH sensitivity of E994K was similar to that of WT TRPM2. These results suggest that changes in the charge of the residues at the outer vestibule play an essential role in the pH_o sensitivity of TRPM2.

Changes of external $[Ca^{2+}]_o$ sensitivity in the pore mutants

The extracellular acidic pH equally inhibited both inward and outward currents of WT TRPM2 and its mutants (Figs. 1 B and 6), suggesting that protons may not simply block the currents at the channel pore; instead, they may change TRPM2 channel gating properties through the residues of H958, D964, and E994. A previous study demonstrated that TRPM2 cannot be activated in the absence of both extracellular and intracellular Ca^{2+} (Starkus et al., 2007), suggesting that external Ca^{2+} is important in TRPM2 gating. Csanády and Törocsik (2009) demonstrated that external Ca^{2+} ($[Ca^{2+}]_o$) activates TRPM2 by binding in deep crevices near the pore but intracellularly of the gate. We have shown in Fig. 3 A that TRPM2 is more sensitive to external proton inhibition at a decreased external Ca^{2+} concentration ($[Ca^{2+}]_o$). To investigate whether external protons alter TRPM2 channel gating via changing the sensitivity of TRPM2 to $[Ca^{2+}]_o$, we tested channel activation and inactivation of WT TRPM2, H958Q, D964N, and E994Q at various external Ca^{2+} concentrations by using a pipette solution

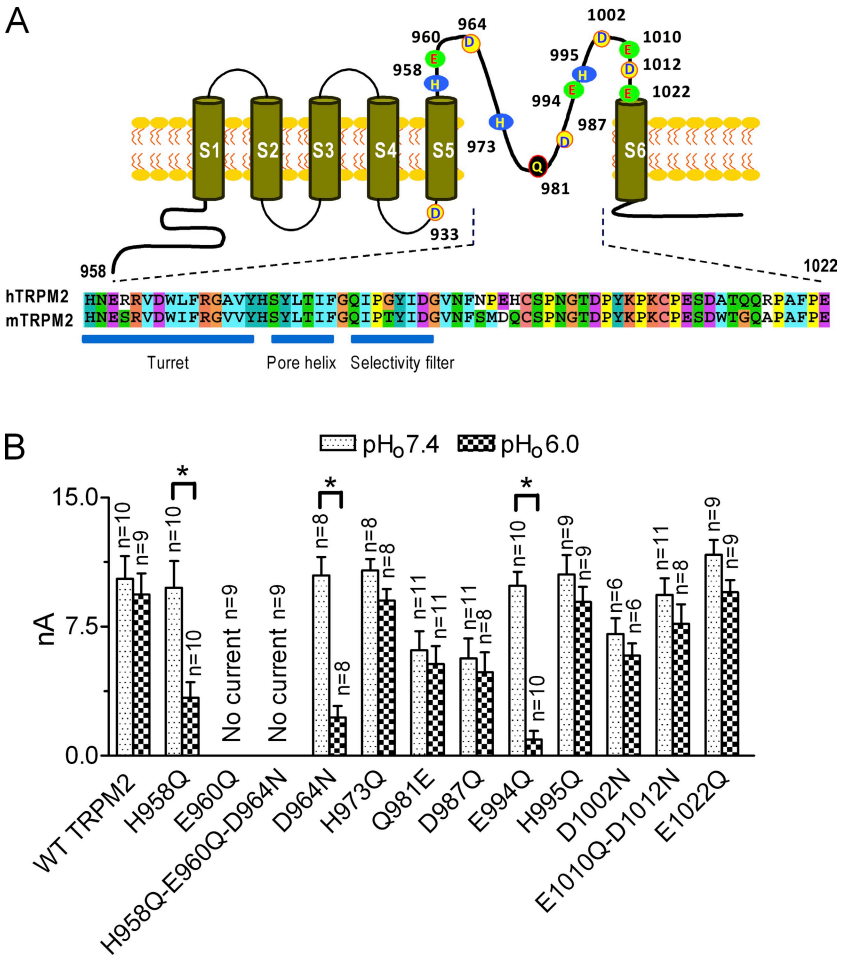

Figure 5. Molecular basis for TRPM2 sensitivity to acidic pH_o. (A) Schematic structure of TRPM2 and positions of substituted amino acid residues in the putative pore region of hTRPM2 (top). Alignment of the residues in the putative pore region of mTRPM2 and hTRPM2 (bottom). (B) Average current amplitude of WT TRPM2 and the mutants at pH_o 7.4 and 6.0. TRPM2 currents were elicited by voltage ramps, and the outward currents at +100 mV were measured. E960Q and the triple mutant H958Q-E960Q-D964N were nonfunctional channels. *, $P < 0.05$.

containing 500 µM ADPR with minimal Ca^{2+} level buffered by 10 mM EGTA. As illustrated in Fig. 7, extracellular divalent-free ($[Ca^{2+}]_o$, <1 nM) solution was not able to activate TRPM2 in the absence of intracellular Ca^{2+}, which is consistent with a previous report (Starkus et al., 2007). The minimal external Ca^{2+} concentration required to activate WT TRPM2 was 10 µM, whereas 150 µM Ca^{2+} was required to activate H958Q, D964N, and E994Q. The EC_{50}s of $[Ca^{2+}]_o$ for H958Q, D964N, and E994Q were significantly increased compared with that for

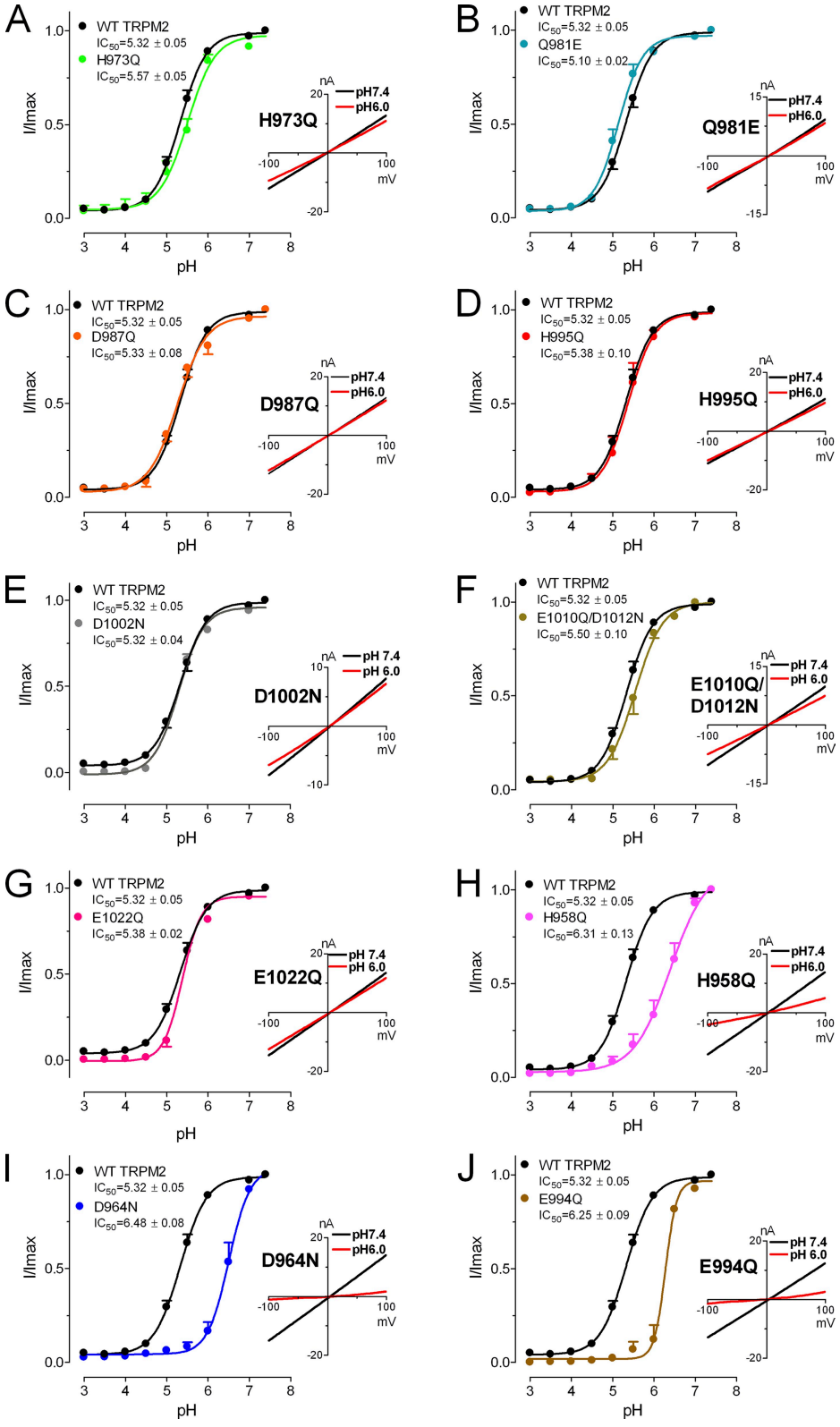

Figure 6. Changes in the pH_o sensitivity of TRPM2 mutants. (A–G) Dose–response curves of the effects of acidic pH_o on mutants H973Q, Q981E, D987Q, H995Q, D1002N, E1010Q/D1012N, and E1022Q. Current amplitudes at the indicated pHs were normalized to the maximal current amplitude at pH_o 7.4. Inset panels illustrate original recordings of WT TRPM2 and the mutants at pH 7.4 and 6.0. Best fit of the dose–response curves yielded IC_{50}s for the mutants indistinguishable from that of WT TRPM2. (H–J) Altered pH_o sensitivity in H958Q, D964N, and E994Q compared with WT TRPM2. Dose–response curves were rightward shifted, and the IC_{50}s were changed by ~1 pH unit for H958Q, D964N, and E994Q, respectively. Inset panels illustrate representative recordings at pH 7.4 and 6.0. Note that the linear I-V relation of WT TRPM2 was not changed in H958Q, D964N, and E994Q. The Hill coefficient was n_H = 1.4 ± 0.1 for WT TRPM2, n_H = 1.0 ± 0.1 for H958Q, n_H = 1.7 ± 0.3 for D964N, and n_H = 3.2 ± 0.3 for E994Q.

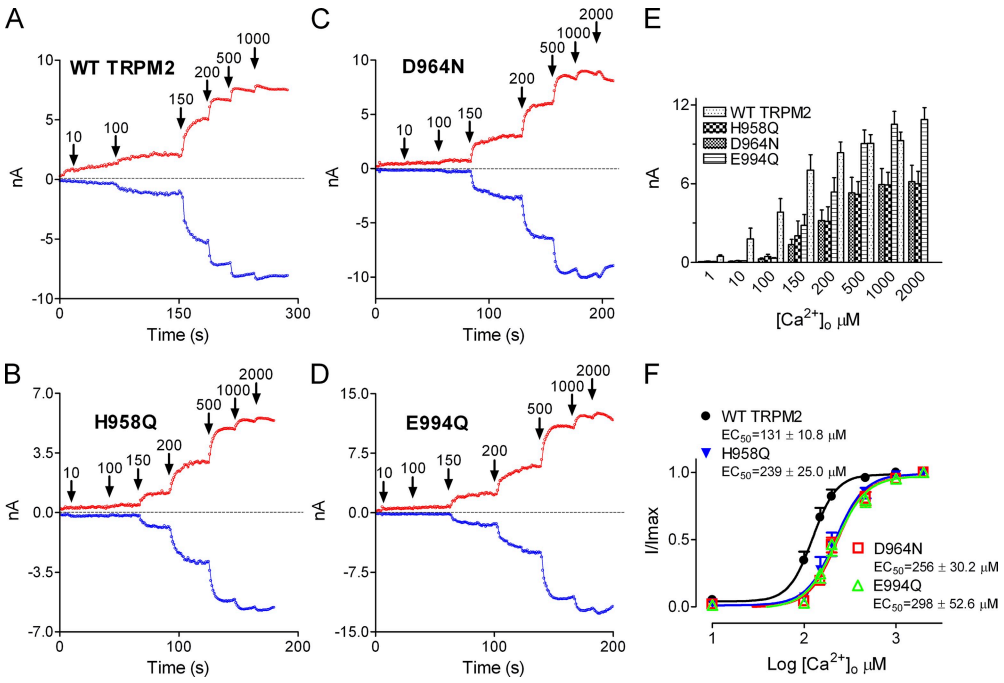

Figure 7. Changes in $[Ca^{2+}]_o$ sensitivity of TRPM2 mutants H958Q, D964N, and E994Q. (A–D) Inward and outward currents of WT TRPM2 (A), H958Q (B), D964N (C), and E994Q (D) activated by the indicated $[Ca^{2+}]_o$. (E) Mean current amplitude of WT TRPM2, H958Q, D964N, and E994Q at the indicated $[Ca^{2+}]_o$. (F) Concentration-dependent effects of $[Ca^{2+}]_o$. Currents were normalized to the maximal value obtained at 2 mM $[Ca^{2+}]_o$. EC_{50}s for Ca^{2+}-mediated activation were 131 ± 10.8 μM ($n_H = 3.3 \pm 0.5$; $n = 8$) for WT TRPM2, 239 ± 25 μM (n_H = 2.7 ± 0.5; n = 8) for H958Q, 256 ± 30.2 μM (n_H = 2.8 ± 0.4; n = 8) for D964N, and 298 ± 52.6 μM ($n_H = 2.6 \pm 0.4$; $n = 8$) for E994Q.

WT TRPM2, suggesting that external protons may inhibit TRPM2 by changing $[Ca^{2+}]_o$-mediated TRPM2 gating, presumably by competing with $[Ca^{2+}]_o$ for binding sites.

In addition to the changes of $[Ca^{2+}]_o$ sensitivity, the activation of H958Q and D964N at 0.5 and 2 mM $[Ca^{2+}]_o$ was significantly slower than that of WT TRPM2 (Fig. S2 E). The activation kinetics is closely related to the gating process of TRPM2. For example, under the conditions with low $[ADPR]_i/[Ca^{2+}]_i$ (Kolisek et al., 2005; Du et al., 2009) or low $[Ca^{2+}]_o$ concentrations (nominally $[Ca^{2+}]_o$ free) (Starkus et al., 2007), activation of TRPM2 is significantly delayed. Thus, the delayed activation of the pore mutants supports the notion that external protons inhibit TRPM2 by inhibiting TRPM2 gating. Unlike WT TRPM2, H958Q, D964N, and E994Q also exhibited time-dependent inactivation at higher $[Ca^{2+}]_o$ (Fig. S2). For example, H958Q, D964N, and E994Q completely inactivated within 100∼200 s at 10 mM $[Ca^{2+}]_o$, whereas the WT TRPM2 displayed sustained current after minor inactivation (Fig. S2 F). Although further studies are required to fully understand how external $[Ca^{2+}]_o$ causes H958Q, D964N, and E994Q inactivation at higher concentrations and delayed activation at lower concentrations, these results further indicate that these pH_o-sensitive residues in the pore region are able to alter $[Ca^{2+}]_o$ sensitivity and therefore regulate TRPM2 channel activation and inactivation.

Changes in single-channel conductance in the pore mutants

To further understand the mechanisms of external protons' inhibition of TRPM2, we investigated the single-channel conductance of the mutants with changed pH_o sensitivity. As shown in Fig. 8, the single-channel conductance was decreased from 75.4 pS (WT TRPM2) to 59.9 pS (D964K), 49.5 pS (E994Q), and 57.8 pS (H958Q), respectively. Moreover, the number of open channels in these mutants was also smaller than that of WT TRPM2. However, due to the fast rundown of single-channel currents, we did not analyze NP_o for the mutants. Nonetheless, the decreased single-channel conductance of the mutants is similar to the single-channel conductance of WT TRPM2 at pH 5.5 (Fig. 2), suggesting that these three residues play an essential role in mediating acidic external pH_o effects on TRPM2.

To summarize, we have shown that extracellular protons inhibit TRPM2 gating by decreasing single-channel conductance. We found that extracellular protons affect extracellular but not intracellular Ca^{2+} sensitivity. Mutations of three extracellular residues change $[pH]_o$ sensitivity and $[Ca^{2+}]_o$ sensitivity, and can mimic the changes of single-channel conductance of the WT TRPM2 induced by acidic pH_o. These results suggest that acidic $[pH]_o$ inhibits TRPM2 by altering $[Ca^{2+}]_o$-mediated TRPM2 gating.

Effects of intracellular protons on TRPM2

To study whether low intracellular pH influences TRPM2 channel activation, we first recorded TRPM2 whole cell currents using intracellular pipette solutions with various proton concentrations. As illustrated in Fig. 9 A, pH_i 6.5 significantly delayed channel activation and decreased current amplitude. At pH_i 5.5, TRPM2 could only be activated for a short time after a long delay (Fig. 9, A and B). The effect of pH_i was reversed upon perfusion with 30 mM NH_4Cl (Fig. 9, C and D), which may

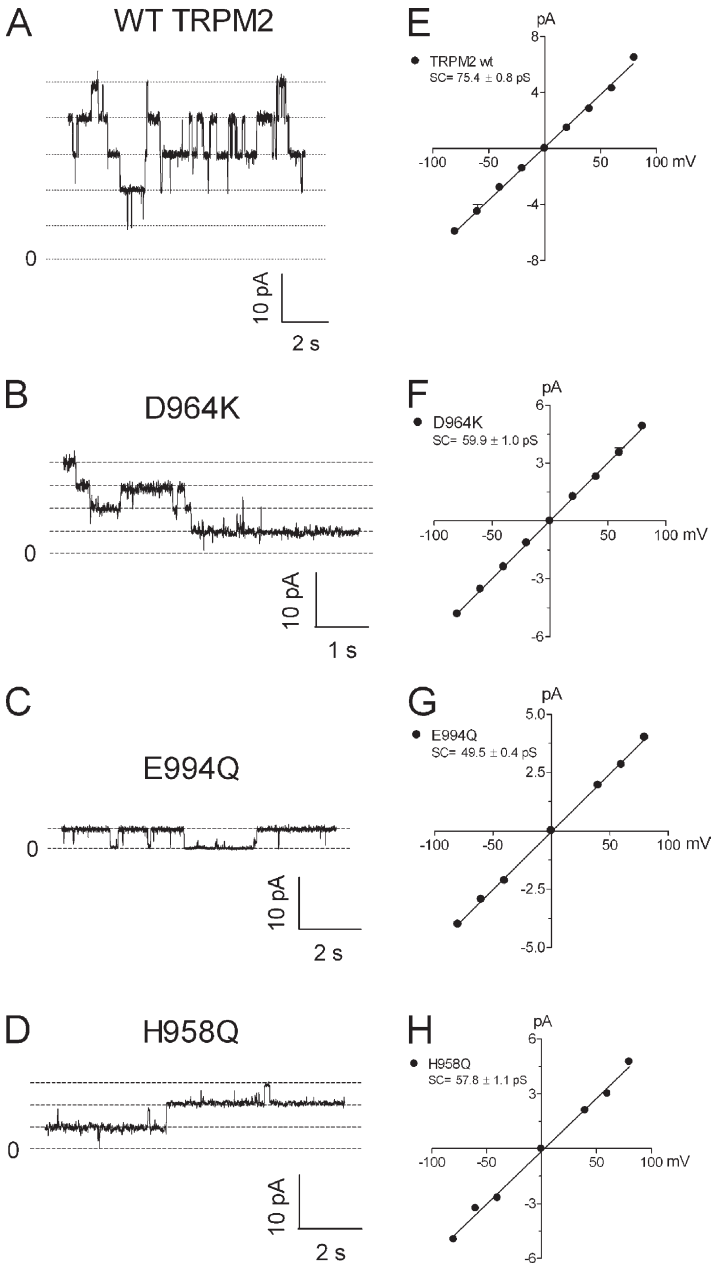

Figure 8. Single-channel conductance of D964K, E994Q, and H958Q. (A–D) Representative recordings of single-channel openings of WT TRPM2, D964K, E994Q, and H958Q at +80 mV in inside-out patches. The external (pipette) solution was normal Tyrode's solution; the internal (bath) solution was nominal Ca^{2+}-free solution with 200 μM ADPR. (E–H) Single-channel conductances obtained by linear regression of single-channel current amplitude at the indicated voltages. The conductance is 59.9 ± 1.0 pS for D964K (n = 8), 49.5 ± 0.4 pS (n = 4) for E994Q, and 57.8 ± 1.1 pS (n = 4) for H958Q.

change intracellular pH by ~2 pH units (Rajdev and Reynolds, 1995). To understand the mechanism of TRPM2 inhibition by pH_i, we tested the effects of various proton concentrations on channel openings in inside-out excised patches. As shown in Fig. 10 A, pH_i 6.5 effectively decreased the number of open channels, and pH_i 5.5 almost completely inhibited all the channel openings. The inhibitory effect of acidic pH was partially reversed when the patches were exposed to high pH solutions (Fig. 10 A). The single-channel conductance was not changed by acidic pH_i (Fig. 10, B–D, right panels). For example, the current amplitude at +80 mV was 6.13 ± 0.02 pA (n = 10) at pH_i 6.5, producing an estimated single-channel conductance of 76.6 pS. At pH_i 5.5, single-channel conductance estimated from the mean current amplitude (6.06 ± 0.02 pA at +80 mV; n = 10) was 75.7 pS. Concentration-dependent effects of internal protons were further evaluated by macroscopic currents obtained from inside-out patches. The IC_{50} of internal protons on TRPM2 was 6.7 pH units (Fig. 10 E), which is close to the pH_i ranges that occur under ischemic pathological conditions (Siesjö, 1988).

Internal protons influence $[Ca^{2+}]_i$- and $[ADPR]_i$-mediated TRPM2 gating

We next investigated the potential mechanism of intracellular protons' effects on TRPM2. TRPM2 currents were recorded in inside-out patches in the bath (internal) solutions containing 200 μM $[ADPR]_i$ and 100 μM or 100 nM $[Ca^{2+}]_i$ at various proton concentrations. As shown in

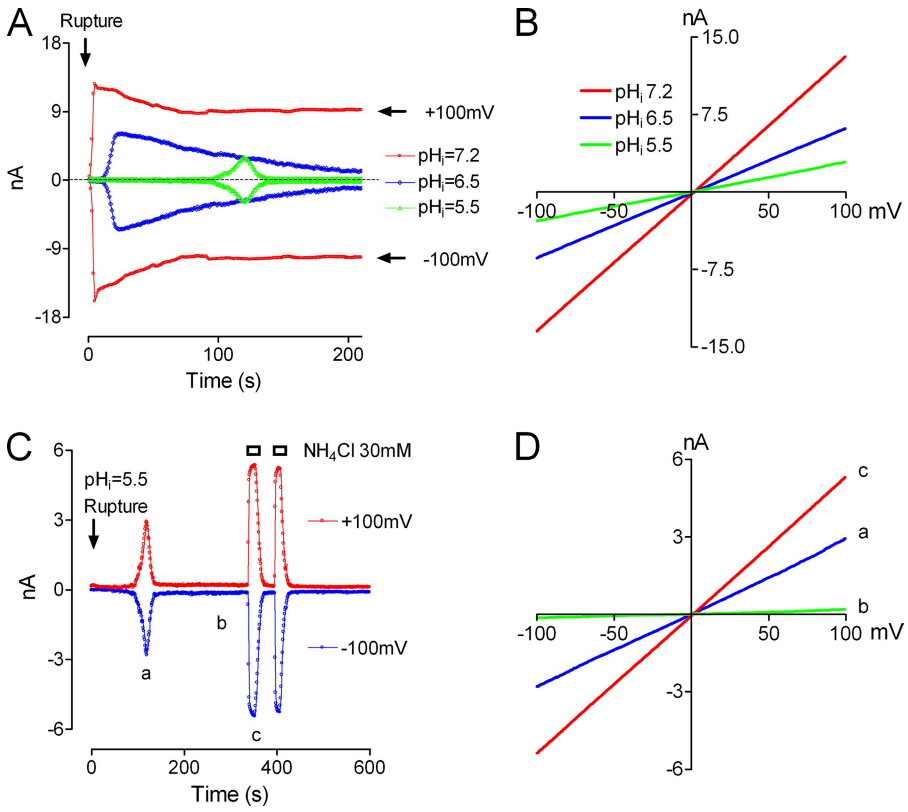

Figure 9. Effects of acidic pH_i on TRPM2 whole cell currents. (A) TRPM2 currents recorded at pH_i 7.2, 6.5, and 5.5. Note that there was a delay for activation of TRPM2 at pH_i 6.5, and a much longer delay for TRPM2 activation at pH_i 5.5. (B) Typical I-V relationship of TRPM2 whole cell current at different pH_is. (C) The inhibitory effect of pH_i 5.5 on TRPM2 was reversed by perfusing the cells with extracellular solutions containing 30 mM NH_4Cl. (D) Representative recordings of TRPM2 in the presence of NH_4Cl. NH_4Cl increased both inward and outward currents of TRPM2.

Fig. 11 A, the IC_{50} was changed from pH_i 6.7 at 100 nM $[Ca^{2+}]_i$ to pH_i 6.3 at 100 μM Ca^{2+}, suggesting that internal protons may compete with $[Ca^{2+}]_i$ for a binding site. To understand how internal protons affect $[ADPR]_i$-mediated TRPM2 activation, we evaluated concentration-dependent effects of ADPR at pH_i 7.2 and 6.7. The ADPR concentration required for activating 50% of the maximal TRPM2 currents was increased from 2.7 to 154.2 ± 27 μM (Fig. 11 B), and the maximal response at pH_i 6.7 is ~30% smaller than that at pH_i 7.2, indicating that both ADPR binding to the binding domain and the coupling between the binding and the channel gating are influenced by acidic pH_i. Therefore, intracellular protons inhibit TRPM2 by altering $[ADPR]_i$-mediated TRPM2 gating.

Molecular mechanisms of intracellular pH sensitivity of TRPM2

To investigate the molecular mechanisms of pH_i regulation on TRPM2, we mutated several titratable intracellular residues at the S2-S3 and S4-S5 linkers and the C terminus adjacent to the S6 domain. Among these mutants, we found that D933N produced dramatic functional changes of TRPM2. With the regular intracellular pipette solutions containing 100 nM $[Ca^{2+}]_i$ and 200 μM $[ADPR]_i$, D933N could not be activated (Fig. 12 B). However, an increase of intracellular Ca^{2+} to 100 μM and ADPR to 1 mM was able to activate D933N (Fig. 12, C and G). The I-V relation of D933N elicited by 100 μM $[Ca^{2+}]_i$/1 mM $[ADPR]_i$ (Fig. 12 G) was similar to that of WT TRPM2 activated by 100 nM Ca^{2+}/200 μM ADPR (Fig. 12 D), although the current amplitude of D933N was smaller than that of WT TRPM2. The requirement of high concentrations of $[Ca^{2+}]_i$ and $[ADPR]_i$ for D933N activation indicates that D933N has decreased sensitivity to $[Ca^{2+}]_i$ and/or $[ADPR]_i$.

To study whether the charge or the side chain of D933 is responsible for the changed characteristics of the channel, we mutated D933 to different residues (Fig. 12, B and C), including D933E, D933H, D933K, and D933A. Using regular pipette solution containing 100 nM Ca^{2+}/200 μM ADPR, we found that only D933E was activated to a small degree (Fig. 12 B), suggesting that the negative charge plays a role in TRPM2 activation. With increased Ca^{2+} and ADPR concentrations (100 μM $[Ca^{2+}]_i$/1 mM $[ADPR]_i$) in the internal pipette solution, both D933E and D933N were substantially activated, although the maximal current amplitudes were much smaller than that of WT TRPM2 (Fig. 12, B and C). D933K and D933H were also activated by the pipette solution containing 100 μM $[Ca^{2+}]_i$/1 mM $[ADPR]_i$. However, the current amplitude of D933K and D933H was only ~10% of that of D933N (Fig. 12 C). Interestingly, D933E and D933H displayed strong outward rectification, with smaller inward currents than that of D933N and WT TRPM2, suggesting that D933E and D933H may have changed TRPM2 gating properties or permeation properties. The mutant D933A produced extremely small currents with a linear I-V

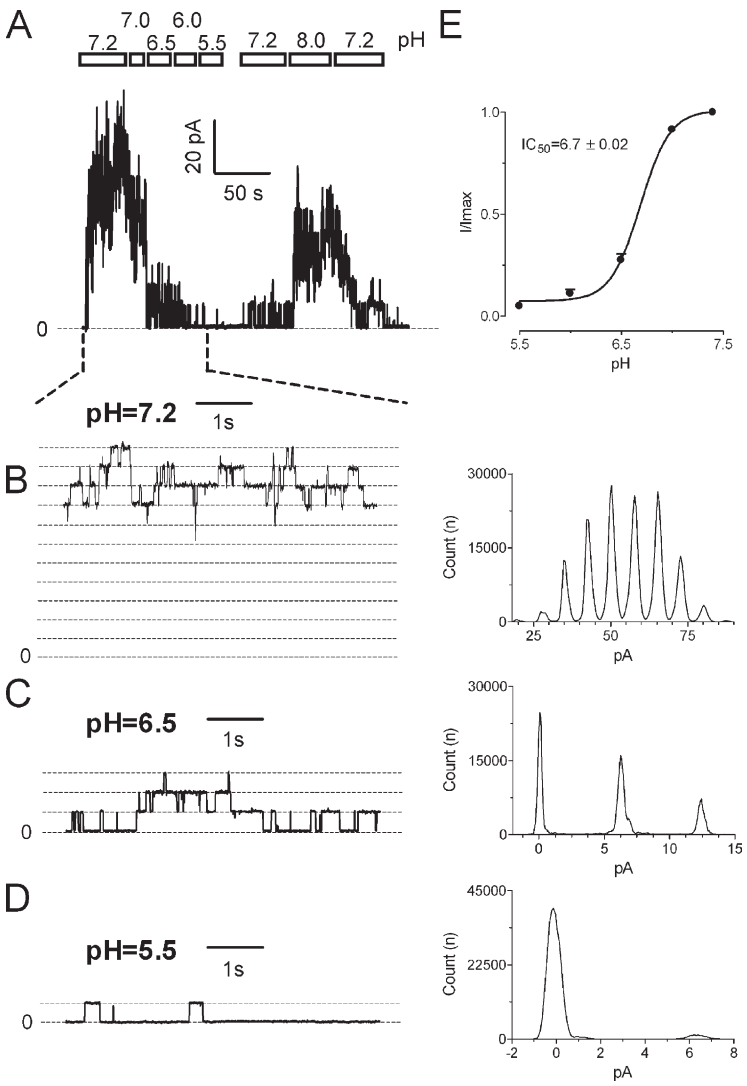

Figure 10. TRPM2 is an intracellular acidic pH sensor. (A) Effects of low pH_i on single-channel currents of TRPM2 obtained from inside-out patches. Single-channel currents were recorded at +80 mV, with the pipette solution containing 2 mM $[Ca^{2+}]_o$ (external solution) and the bath solution (internal solution) containing 100 nM $[Ca^{2+}]_i$ and 200 μM $[ADPR]_i$. Intracellular low pH blocked TRPM2 channel openings (+80 mV), and the effect was partially reversed by pH_i 8.0. (B–D) Single-channel currents recorded at the indicated pH_is. Current amplitude histograms illustrate the number of open channels (right). (B) At pH_i 7.2, there were >10 open channels. (C) At pH_i 6.5, the number of open channels decreased to two. Average current amplitude (6.13 ± 0.02 pA; $n = 10$) estimated a single-channel conductance of 76.6 pS. (D) Channel opening was almost eliminated at pH_i 5.5. Single-channel conductance estimated from the mean current amplitude (6.06 ± 0.02 pA; $n = 10$) was 75.7 pS. (E) Concentration-dependent effects of internal protons on TRPM2. Macroscopic currents of TRPM2 were obtained in inside-out patches. A best fit of the normalized current amplitude yielded an IC_{50} of 6.7 ± 0.02 pH units ($n_H = 3.0 \pm 0.3$; $n = 10$ for each indicated pH). Analysis using currents recorded at +80 mV or at −80 mV produced identical IC_{50}s.

relation. Moreover, D933E, D933N, and D933H displayed strong time-dependent inactivation (Fig. 12 A). Currents were almost completely inactivated within 150 s (Fig. 12 A). These results indicate that both the charge and the side chain of the residues contributed to the changed I-V relation, $[ADPR]_i/[Ca^{2+}]_i$ sensitivity, and gating properties of the TRPM2 mutants at the position of D933.

Using pipette solutions containing 100 μM $[Ca^{2+}]_i$/1 mM $[ADPR]_i$, we further tested intracellular pH effects on D933N and D933E, but not D933H, D933K, and D933A due to their small current amplitude. Internal pH_i 6.0 did not inhibit D933N or D933E, whereas WT TRPM2 was blocked by 80% at pH_i 6.0 (Fig. 13, A–F). At pH_i 5.0, however, D933N and D933E were blocked by 70% (Fig. 13, C–F). Concentration-dependent effects illustrated that IC_{50}s of protons on D933N and D933E were changed from pH_i 6.3 (WT TRPM2) to pH_i 5.5 and 5.3, respectively (Fig. 13, G and H). In addition, the maximal current amplitude of D933N (0.7 ± 0.1 nA/pF; $n = 9$) and D933E (0.9 ± 0.05; $n = 12$) at pH_i 7.2 was much smaller than that of WT TRPM2 (1.1 ± 0.04 nA/pF; $n = 6$). These results indicate that D933 is responsible for the intracellular proton sensitivity of TRPM2.

Overall, although neutralization of D933 did not completely eliminate pH_i sensitivity, the IC_{50} for intracellular protons of D933N is significantly decreased compared with that of WT TRPM2. Moreover, several lines of evidence suggest that D933N can mimic the protonated state of WT TRPM2, including: (1) slow activation and inactivation of D933N (Fig. 12 A, blue) is similar to that of WT TRPM2 at pH_i 6.5 (Fig. 9 A, blue); (2) changed sensitivity to $[Ca^{2+}]_i$ and/or $[ADPR]_i$ of D933N (Fig. 12) is also similar to the effects of $[Ca^{2+}]_i$ and $[ADPR]_i$ on TRPM2 at acidic pH_i; and (3) the maximal current amplitude of D933N at 100 μM $[Ca^{2+}]_i$/1 mM $[ADPR]_i$ is smaller than that of WT TRPM2 (Fig. 13, A–D), which is similar to the decreased maximal current amplitude of WT TRPM2 (100 nM $[Ca^{2+}]_i$/1 mM $[ADPR]_i$) at pH_i 6.7 compared with that of pH_i 7.2 (Fig. 11 B). Although D933 may form a Ca^{2+} binding site by coordinating with surrounding residues, given the similar characteristics of D933E and D933N, our data indicate that D933 plays

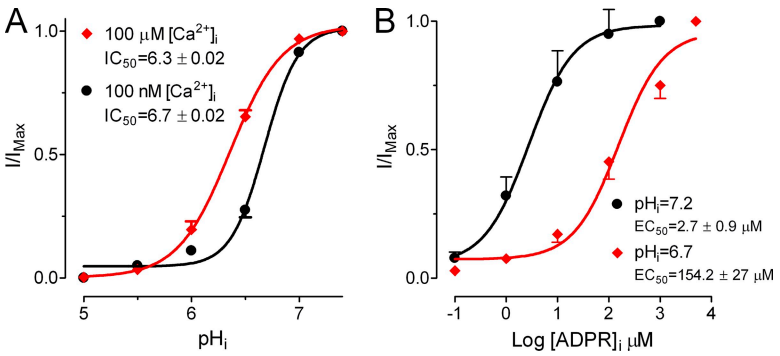

Figure 11. Effects of internal protons on $[Ca^{2+}]_i$- and $[ADPR]_i$-induced TRPM2 gating. (A) Concentration-dependent effects of internal protons on TRPM2 at various concentrations of internal $[Ca^{2+}]_i$. TRPM2 currents were elicited by voltage ramps (−100 to +100 mV; HP = 0 mV) under inside-out configuration, and the macroscopic current amplitude was measured at +100 mV. The intracellular solution (bath solution) contained 200 μM ADPR with 100 μM or 100 nM Ca^{2+}; the external solution (pipette solution) was normal Tyrode's solution containing 2 mM Ca^{2+}. Best fit of normalized current yielded an IC_{50} of 6.7 ± 0.02 (n = 10) at 100 nM $[Ca^{2+}]_i$ and 6.3 ± 0.02 (n = 11; P < 0.01) at 100 uM $[Ca^{2+}]_i$. (B) Effects of internal low pH_i on $[ADPR]_i$-induced TRPM2 gating. Macroscopic currents were recorded using inside-out patches by voltage ramps (−100 to +100 mV; HP = 0 mV) in the nominal Ca^{2+}-free (~10 μM) internal solutions at pH_i 7.2 or 6.7 with various concentrations of ADPR. The EC_{50}s of ADPR were 2.7 ± 0.9 μM (n = 5) at pH_i 7.2 and 154.2 ± 27 μM at pH_i 6.7 (n = 5).

an essential role in intracellular pH_i sensitivity and in intracellular $[Ca^{2+}]_i$/$[ADPR]_i$-mediated TRPM2 gating. Furthermore, because the residue D933 is located in the S4-S5 linker, it may be an important component of the intracellular gate of TRPM2. Additionally, it is plausible that D933 may serve as the binding site for external $[Ca^{2+}]_o$ permeating through the channel; therefore, D933 may be able to regulate external $[Ca^{2+}]_o$-mediated TRPM2 gating.

DISCUSSION

We demonstrate that TRPM2 is regulated by both extracellular and intracellular acidic conditions. While acidic pH_o inhibits TRPM2 by decreasing single-channel conductance, acidic pH_i blocks TRPM2 by inducing channel closure without changing channel conductance. We identify three external residues that are responsible for external pH_o sensitivity as well as external $[Ca^{2+}]_o$ sensitivity. Mutations of the three residues decrease single-channel conductance, change pH_o sensitivity, and reduce $[Ca^{2+}]_o$ affinity to TRPM2. Because the three residues are located at the outer vestibule of the pore, it seems that protonation of these residues causes conformational changes leading to alteration of TRPM2 gating and/or causes decreased Ca^{2+} permeation, therefore inhibiting $[Ca^{2+}]_o$-mediated TRPM2 gating. We find that the intracellular residue D933 at the C terminus of the S4-S5 linker is responsible for acidic pH_i sensitivity. Moreover, mutations of D933 significantly inhibit intracellular $[Ca^{2+}]_i$- and $[ADPR]_i$-mediated TRPM2 gating, suggesting that D933 could be an important component of the intracellularly of the gate for TRPM2 gating. Collectively, our results not only reveal a novel mechanism of TRPM2 modulation by internal and external protons, but also provide molecular mechanisms for acidic pH modulation of TRPM2.

TRPM2 is inhibited by internal and external acidic pH

TRPM2 is a Ca^{2+}-permeable nonselective cation channel that can be activated by ADPR, cADPR, NAD^+, oxidative stress, and an increase of temperature (Perraud et al., 2001; Sano et al., 2001; Hara et al., 2002; Beck et al., 2006; Togashi et al., 2006). ADPR, cADPR, and intracellular Ca^{2+} can produce synergized activation of TRPM2, leading to maximal activation of the channel and resulting in cell death via Ca^{2+} overload. Interestingly, TRPM2 is also involved in insulin secretion (Togashi et al., 2006) and inflammatory responses (Yamamoto et al., 2008), suggesting that other regulatory mechanisms are involved in TRPM2 gating. We demonstrate that extracellular and intracellular acidic pH effectively inhibits TRPM2 channel activity (Figs. 1 and 10). Thus, acidic pH may serve as a negative feedback to control TRPM2 gating under physiological or pathological conditions. A recent study demonstrated that TRPM2 is involved in regulating reactive oxygen species–induced chemokine production in monocytes, thereby aggravating inflammation (Yamamoto et al., 2008). It is known that local tissue acidosis occurs during inflammation, ischemia, or tissue injury. Therefore, the inhibitory effects of acidic pH on TRPM2 may slow down the deteriorating process of a cell caused by TRPM2 activation during reactive oxygen species–associated inflammation or during ischemia, and therefore sustain the inflammatory status. Nonetheless, it is plausible that the regulatory effects of acidic pH on TRPM2 gating may also confer some unknown physiological or pathological functions.

Extracellular acidification has been shown to regulate the activity of a large number of ion channels, including several TRP channels. Extracellular acidic pH is involved in TRPV1 channel gating (Jordt et al., 2000; Ryu et al., 2003), potentiates TRPC4 and TRPC5 currents but inhibits TRPC6 currents (Semtner et al., 2007), blocks Ca^{2+}-activated TRPM5 (Liu et al., 2005), inhibits TRPV5 (Yeh et al., 2003), and potentiates TRPM6 and TRPM7 inward currents (Jiang et al., 2005; Li et al., 2006, 2007). Internal protons inhibit TRPM7 by screening negative charges of PIP_2 (Kozak et al., 2005) and block TRPM8 activated by icilin or low temperature (Andersson et al., 2004). Here, we show that TRPM2 is inhibited by both internal and external protons. Although our data suggest that both internal and external protons inhibit TRPM2 by altering its

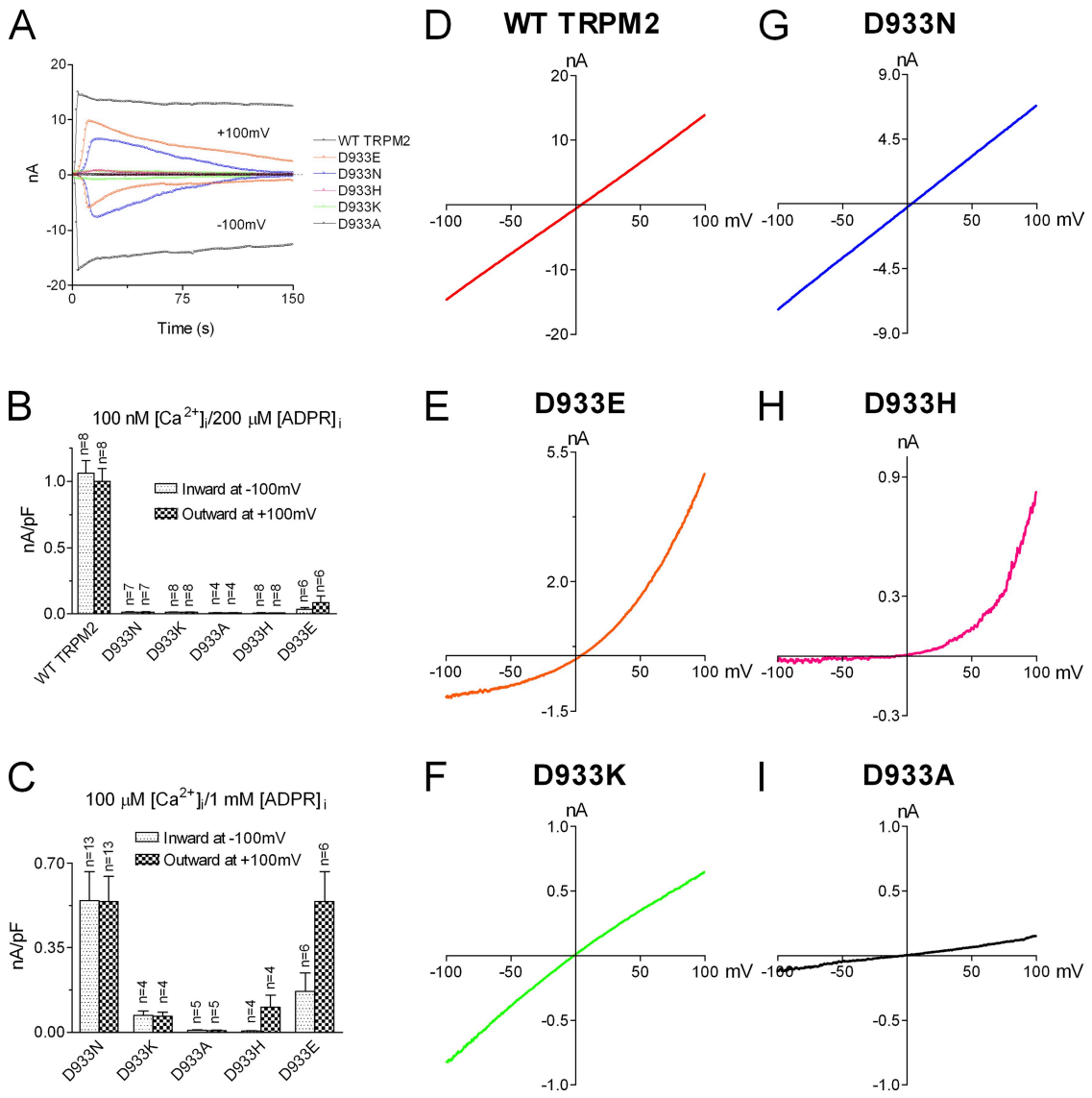

Figure 12. An intracellular residue, D933, influences TRPM2 channel gating. (A) Current amplitude measured at +100 and −100 mV of D933E, D933N, D933H, D933K, and D933A compared with WT TRPM2. The mutant channels were activated by intracellular solutions containing 100 μM Ca^{2+} and 1 mM ADPR, whereas WT TRPM2 was activated by 100 nM Ca^{2+}/200 μM ADPR. Note that D933E and D933N quickly inactivated after activation. (B) Mean current amplitude of WT TRPM2 and the mutants recorded with 100 nM Ca^{2+}/200 μM ADPR. (C) Mean current amplitude of the mutants activated by 100 μM Ca^{2+}/1 mM ADPR. (D–I) I-V relationship of D933N, D933E, D933H, D933K, and D933A compared with that of WT TRPM2. Both D933E and D933H displayed smaller inward currents than that of D933N.

gating properties, there are several differences between internal and external proton-induced inhibition of TRPM2. For example, the IC_{50} of pH_i (IC_{50} = 6.7 pH units) is much higher than that of pH_o (IC_{50} = 5.3 pH units). Although the block induced by internal protons can be readily reversed by high pH_i (Figs. 9 and 10), blocking of TRPM2 by pH_o = 4.0 is not reversible. In addition, extracellular protons decrease channel conductance (Fig. 2), whereas intracellular protons inhibit TRPM2 by efficiently leading to channel closure without altering channel conductance (Fig. 10). These different effects suggest that internal and external protons regulate TRPM2 channel activities via distinctive mechanisms.

Molecular mechanisms of extracellular pH sensitivity of TRPM2

We demonstrate that acidic pH_o equally inhibits inward and outward currents of TRPM2 in a voltage-independent manner (Fig. 1), suggesting that external protons may alter gating properties of TRPM2. How could external protons affect TRPM2 gating properties? Although the detailed gating mechanisms of TRPM2 are to be established, it is known that TRPM2 can be activated by intracellular ADPR (Perraud et al., 2001, 2005; Sano et al., 2001; Kühn and Lückhoff, 2004) or by intracellular $[Ca^{2+}]_i$ in the absence of $[ADPR]_i$ (Du et al., 2009). Moreover, a recent study demonstrated that external

Ca^{2+} activates TRPM2 channels by binding to the activating site intracellularly of the gate (Csanády and Törocsik, 2009). Therefore, it is possible that extracellular protons inhibit TRPM2 by altering $[Ca^{2+}]_o$-mediated TRPM2 gating. Indeed, using the conditions modified from a previously study (Starkus et al., 2007) that allow extracellular Ca^{2+} to activate TRPM2, we found that the external proton concentration for inhibiting 50% TRPM2 at 2 mM $[Ca^{2+}]_o$ is significantly higher than that at 200 µM $[Ca^{2+}]_o$ (Fig. 3 A), indicating that external protons compete with $[Ca^{2+}]_o$ for binding sites.

Do external protons permeate through TRPM2 to compete with $[Ca^{2+}]_o$ for the binding site intracellularly of the gate (Csanády and Törocsik, 2009)? Several lines of evidence suggest that external protons do not permeate through TRPM2. First, when the proton is the only cation (besides $NMDG^+$) in the external solutions, proton currents could not be elicited by holding the cells at −100 mV (Fig. 4, A and B) or by voltage ramps (−100 to +100 mV) using the pipette conditions that favor proton conductivity (Fig. 4, C and D) (Numata and Okada, 2008). Second, the IC_{50} obtained at HP = 0 mV was not

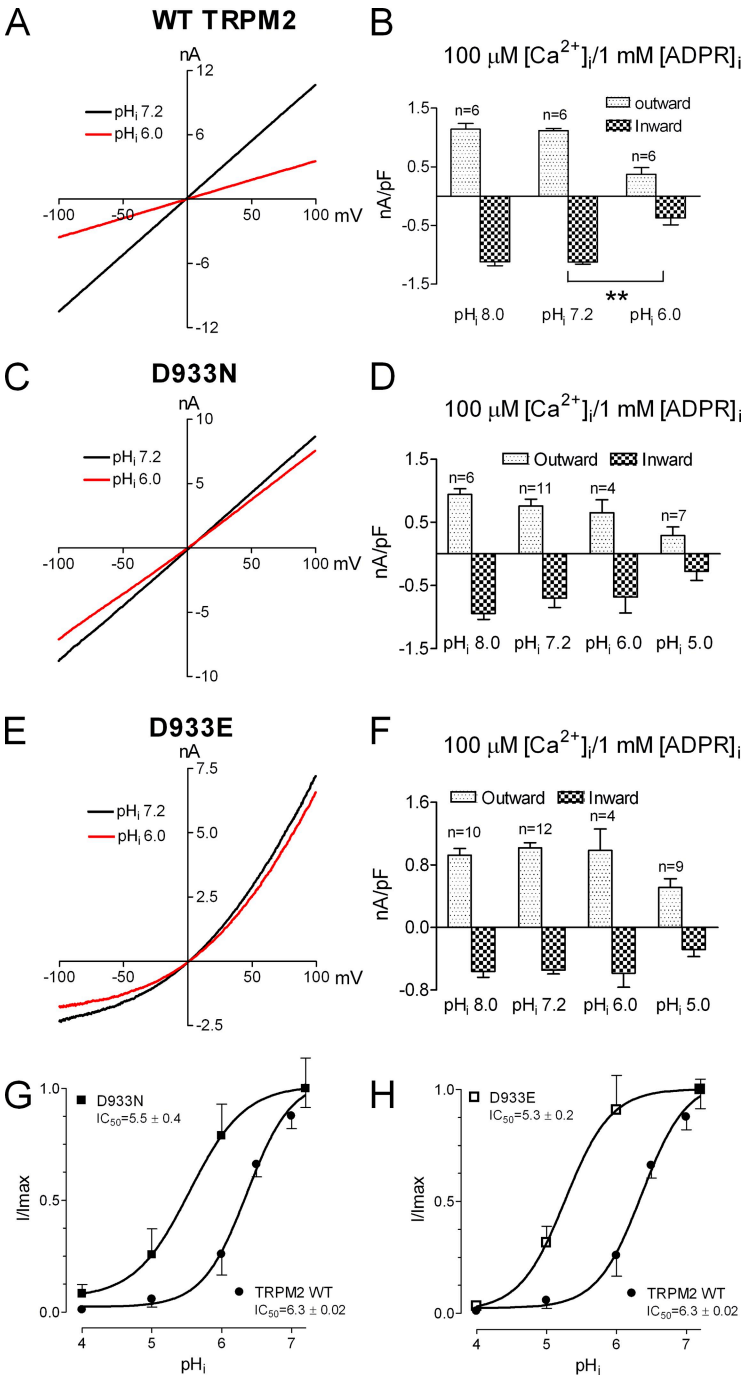

Figure 13. D933 is an intracellular pH sensor. (A and B) WT TRPM2 activated by 100 µM $[Ca^{2+}]_i$/1 mM $[ADPR]_i$ was largely blocked at pH_i 6.0. (C and D) Effects of acidic pH_i on D933N activated by 100 µM $[Ca^{2+}]_i$/1 mM $[ADPR]_i$. Acidic pH_i 6.0 did not change current amplitude, whereas pH_i 5.0 significantly inhibited D933N currents. (E and F) Effects of pH_i on D933E. A significant decrease in current amplitude was observed at pH 5.0, but not pH 6.0. (G and H) Concentration-dependent effects of acidic pH_i on D933N and D933E. IC_{50}s obtained by best fit of the dose–response curves were 5.5 ± 0.4 pH units for D933N and 5.3 ± 0.2 pH units for D933E. **, $P < 0.01$.

significantly different from that obtained at HP = −100 mV; the latter would favor proton permeation. Third, an increase in intracellular pH_i by perfusing the cells with 30 mM NH_4Cl could not reverse the inhibition of TRPM2 induced by pH_o 4.0 (Fig. 4 F), whereas 30 mM NH_4Cl perfusion effectively reversed the inhibition of TRPM2 produced by low pH_i (Fig. 9 C). Fourth, $[Ca^{2+}]_i$ did not change the IC_{50} of external protons on TRPM2 (Fig. 3 B). Thus, it appears unlikely that external protons are able to inhibit TRPM2 channel activities by competing with $[Ca^{2+}]_o$ for a binding site on the cytoplasmic side.

To determine the molecular mechanism by which external protons inhibit TRPM2, we mutated all the titratable residues between S5 and S6 to determine which sites are responsible for pH_o sensitivity. The mutants at the putative selectivity filter of TRPM2 (Chubanov et al., 2007; Xia et al., 2008) displayed similar pH sensitivity as the WT TRPM2 (Figs. 5 and 6). Both D987 and Q981 have been shown to increase Ca^{2+} permeability when mutated to glutamate (Xia et al., 2008). However, D987Q and Q981E did not alter pH_o sensitivity (Fig. 6), suggesting that, different from TRPM7 (Li et al., 2007) and voltage-gated Ca^{2+} channels (Chen and Tsien, 1997), competing with Ca^{2+} for binding sites in the selectivity filter does not underlie the mechanisms of pH_o effects on TRPM2. Interestingly, we found that H958Q, D964N, and E994Q significantly changed pH_o sensitivity (Fig. 6) compared with the WT TRPM2. H958 and D964 are located in the putative turret loop upstream of the pore helix, whereas E994 is located downstream of the selectivity filter. It has been shown that His residues in the turret loop of $K_{2p}2.1$ channels can sense pH_o and control channel gating (Cohen et al., 2008). A Glu residue (E600) in the turret loop linking the S5 domain within the putative pore-forming region serves as a key regulatory site of the TRPV1 in response to changes in extracellular pH (Jordt et al., 2000). Therefore, the titratable residues in the turret loop of the outer vestibule play a crucial role in pH_o sensitivity and channel gating. We found that mutations of H958, D964, and E994 not only markedly changed pH_o sensitivity (Fig. 6) and $[Ca^{2+}]_o$ affinity (Fig. 7), but also decreased single-channel conductance of TRPM2, supporting the notion that these three titratable residues at the outer vestibule are the molecular determinants for pH_o sensitivity and are also involved in permeation of TRPM2, presumably via conformational changes of the selectivity filter, thereby ultimately leading to changes of channel gating properties.

How could extracellular protons affect TRPM2 gating? One possibility is that extracellular protons alter TRPM2 gating by reducing $[Ca^{2+}]_o$ sensitivity, therefore inhibiting $[Ca^{2+}]_o$-mediated TRPM2 activation. We demonstrate that in the absence of intracellular Ca^{2+}, a condition that allows $[Ca^{2+}]_o$ to play a major role in TRPM2 activation (Starkus et al., 2007), the EC_{50} of $[Ca^{2+}]_o$ required for TRPM2 activation was changed from 131 µM for WT TRPM2 to 239, 256, and 298 µM for H958Q, D964N, and E994Q, respectively (Fig. 7). Because H958, D964, and E994 are located at the outer vestibule, the significant decrease in $[Ca^{2+}]_o$ affinity suggests that external protons compete with $[Ca^{2+}]_o$ for binding sites at the entrance of the pore (Figs. 3 A and 7). Negative charges in the outer vestibule have been shown to be important in maintaining a high concentration of permeating ions, a mechanism that has been demonstrated for other channels, including Na^+ (Khan et al., 2002), K^+ (Nimigean et al., 2003), and Cl^- channels (Middleton et al., 1996). By competing with $[Ca^{2+}]_o$ for the binding sites at the outer vestibule, protons may decrease the accumulation of $[Ca^{2+}]_o$, diminish Ca^{2+} entry, and lead to inhibition of $[Ca^{2+}]_o$-mediated TRPM2 activation. Although the Ca^{2+} conductance of D964K was not significantly smaller than that of WT TRPM2 when isotonic Ca^{2+} was used in the external solution (Fig. S3), it is possible that Ca^{2+} conductance of D964K and other mutants may be markedly reduced at submillimolar $[Ca^{2+}]_o$, thereby resulting in decreased Ca^{2+} permeation. Further experiments are required to compare the Ca^{2+} conductance of the three mutants with that of WT TRPM2 by using submillimolar or physiological $[Ca^{2+}]_o$. Nonetheless, it is conceivable that external protons compete with external $[Ca^{2+}]_o$, affecting the $[Ca^{2+}]_o$-activating site near the intracellular mouth of the channel pore (Csanády and Törocsik, 2009) by decreasing Ca^{2+} entry, thereby leading to inhibition of TRPM2 gating.

The single-channel conductances of D964K, E994Q, and H958Q (Fig. 8) are much smaller than that of WT TRPM2 at pH_o 7.4, but similar to that of WT TRPM2 at pH_o 5.5 (Fig. 2), suggesting that protonation of these residues or mutations of these residues at the outer vestibule might cause conformational change of the selectivity filter, thereby leading to a decrease in cation influx through the pore. Alternatively, protonation or mutations of these residues might reduce overall surface charges in the outer vestibule, resulting in decreased local cation concentrations and hence Na^+ and Ca^{2+} influx, thereby leading to inhibition of TRPM2 channel gating. Further investigation is required to fully understand the detailed mechanisms underlying how external protons regulate TRPM2 channel gating.

Collectively, our results support the following model: external protons compete with $[Ca^{2+}]_o$ for binding sites at the outer vestibule, resulting in a decrease in local Ca^{2+} concentration and/or conformational changes of the selectivity filter, thereby leading to reduced cation influx and inhibition of $[Ca^{2+}]_o$-mediated TRPM2 gating.

Molecular basis for intracellular proton sensitivity of TRPM2

TRPM2 is more sensitive to intracellular than extracellular acidic pH (Figs. 6 and 10). The IC_{50} of intracellular protons needed to inhibit TRPM2 is pH_i 6.7, a pH range that usually occurs under ischemia conditions

(Siesjö, 1988). It has been shown that intracellular protons inhibit TRPM7 by screening negative charges of PIP_2 (Kozak et al., 2005), which is required for TRPM7 channel activity (Runnels et al., 2002). Different from TRPM7, inhibition of TRPM2 by intracellular protons is mediated by a specific amino acid residue (D933), which is located at the C terminus of the S4-S5 linker (Figs. 5 and 10). It is remarkable that replacement of D933 by other residues not only changes pH_i sensitivity, but also alters the ability of $[Ca^{2+}]_i$ and $[ADPR]_i$ to gate TRPM2, indicating that D933 is crucial for TRPM2 gating in addition to its ability as a pH_i sensor. Indeed, replacement of D933 by E933 and H933 alters the I-V relation of TRPM2 by diminishing their inward currents, further supporting that D933 is pivotal in TRPM2 channel gating. D933 is located at the C terminus of the S4-S5 linker. It is known that the S4-S5 linker influences voltage sensor and is involved in the gating of voltage-gated channels (Caprini et al., 2005), including potassium channels (Choe, 2002), HCN channels (Chen et al., 2001), and voltage-dependent TRPM8 (Voets et al., 2007). Here, we provide compelling evidence that the S4-S5 linker is also involved in TRPM2 channel gating. Therefore, our results establish that, besides the N-terminal Ca^{2+}–calmodulin binding domain (Du et al., 2009) and the C-terminal ADPR binding domain (Perraud et al., 2001; Sano et al., 2001), which are crucial in TRPM2 activation, the S4-S5 linker is another important domain contributing to TRPM2 gating.

It appears that both the side chain and the negative charge are crucial for D933 to fit the local microenvironment to support TRPM2 channel activation mediated by $[ADPR]_i$ and $[Ca^{2+}]_i$. Substitution of D933 with various residues virtually renders TRPM2 an inactivated channel under the pipette conditions containing 100 nM $[Ca^{2+}]_i$ and 200 µM $[ADPR]_i$, except for D933E, which can be activated to a small degree (Fig. 12 B), suggesting that the negative charge of D933 is essential for TRPM2 gating. When higher concentrations of $[ADPR]_i$ (1 mM) and $[Ca^{2+}]_i$ (100 µM) are included in the pipette solutions, all the substitution mutants except D933A are activated, although the current amplitudes of D933K and D933H are only one tenth of the current amplitude of D933N or D933E (Fig. 12). These results strongly suggest that the residue D933 contributes to TRPM2 gating by carrying a negative charge as well as by having the right molecular size or side chain to fit the local microenvironment. Because endogenous $[ADPR]_i$ is in the micromole range (Heiner et al., 2006) and $[Ca^{2+}]_i$ is <100 nM, changes in pH_i under pathological ischemic conditions can readily inactivate TRPM2. Therefore, D933 can be an intracellular proton sensor for regulating TRPM2 channel activity.

How could intracellular protons change TRPM2 gating properties through D933 residue? TRPM2 gating is a complex process. Although it is known that $[ADPR]_i$ and intracellular and extracellular Ca^{2+} can activate TRPM2, the detailed mechanisms are not fully understand. For example, it is unknown how $[Ca^{2+}]_i$ synergizes with $[ADPR]_i$ to gate TRPM2 (Perraud et al., 2001; Kolisek et al., 2005), and whether there are direct $[Ca^{2+}]_i$ binding sites besides the Ca^{2+}–calmodulin binding domain (Du et al., 2009). Despite the complexity of gating mechanisms, we demonstrated several lines of evidence that neutralization of D933 can mimic the inhibition of TRPM2 induced by acidic pH_i. First, neutralization of D933 significantly decreased the sensitivity of TRPM2 to $[Ca^{2+}]_i$ and $[ADPR]_i$ (Fig. 12, A–C), and similar effects were observed for the WT TRPM2 at acidic pH_i (Fig. 11). Second, D933N displayed slow activation and time-dependent inactivation (Fig. 12 A), which is similar to the time-dependent activation and inactivation of the WT TRPM2 at pH_i 6.5 (Fig. 9 A). Third, D933N is much less sensitive to intracellular protons compared with the WT TRPM2 (Fig. 13). Thus, the negative charge of D933 plays an essential role in pH_i sensitivity. Furthermore, it seems that the side chain of D933 is also crucial for TRPM2 gating and pH_i sensitivity, as D933E produced similar pH_i sensitivity to that of D933N, but displayed strong rectification characteristics. Several mechanisms may underlie the molecular basis by which intracellular protons inhibit TRPM2 gating. First, protons compete with Ca^{2+} for the binding site; therefore, protonation of D933 leads to inhibition of $[Ca^{2+}]_i$-induced TRPM2 gating, or inhibition of $[ADPR]_i/[Ca^{2+}]_i$-mediated gating by diminishing synergistic effects of $[Ca^{2+}]_i$ and $[ADPR]_i$. Second, it is plausible that D933 could be an important residue intracellularly of the gate, so that titration of D933 may induce conformational changes, leading to inhibition of TRPM2 gating. Intracellular protons have been shown to potentiate CNG channel gating by directly coordinating the interaction of the ligand with an Asp residue in the cytosolic nucleotide binding pocket of the channel, leading to the stabilization of the open state (Gordon et al., 1996). It will be of interest to investigate whether acidic $[pH]_i$ alters $[ADPR]_i$ binding in future studies. Furthermore, it will also be of interest to investigate whether D933 is the binding site for $[Ca^{2+}]_o$ near the intracellular mouth and acts as the $[Ca^{2+}]_o$-activating site to regulate $[Ca^{2+}]_o$-mediated TRPM2 activation. Further investigation is required to test this hypothesis.

Collectively, it appears that D933 is an intracellular Ca^{2+} binding site. Internal protons compete with $[Ca^{2+}]_i$ for binding, therefore inhibiting $[Ca^{2+}]_i$- and $[ADPR]_i$-mediated TRPM2 gating. Alternatively, protonation of D933 may cause conformational changes resulting in alteration of channel characteristics and inhibition of TRPM2 channel activation.

Conclusions

We demonstrate that both intracellular and extracellular protons block TRPM2 by inhibiting TRPM2 channel

gating. The molecular mechanisms by which extracellular protons inhibit TRPM2 gating is through titration of D964, H958, and E994 at the outer vestibule, resulting in conformation changes and inhibition of $[Ca^{2+}]_o$-mediated TRPM2 gating. We identify that the residue D933 at the C terminus of the S4-S5 linker confers pH_i sensitivity as well as regulates $[ADPR]_i/[Ca^{2+}]_i$-mediated TRPM2 gating. Given the physiological significance of TRPM2-mediated Ca^{2+} currents, controlling TRPM2 gating by intracellular and extracellular acidic pH may generate important physiological and/or pathological implications.

We thank Dr. A. Scharenberg and Dr. Y. Mori for providing us the TRPM2 constructs. We thank Drs. Laurinda Jaffe, David Clapham, and Haoxing Xu for constructive suggestions and comments.

This work was partially supported by National Institutes of Health (grant HL078960 to L. Yue).

Edward N. Pugh Jr. served as editor.

Submitted: 4 May 2009
Accepted: 21 October 2009

REFERENCES

Andersson, D.A., H.W. Chase, and S. Bevan. 2004. TRPM8 activation by menthol, icilin, and cold is differentially modulated by intracellular pH. *J. Neurosci.* 24:5364–5369. doi:10.1523/JNEUROSCI.0890-04.2004

Beck, A., M. Kolisek, L.A. Bagley, A. Fleig, and R. Penner. 2006. Nicotinic acid adenine dinucleotide phosphate and cyclic ADP-ribose regulate TRPM2 channels in T lymphocytes. *FASEB J.* 20:962–964. doi:10.1096/fj.05-5538fje

Caprini, M., M. Fava, P. Valente, G. Fernandez-Ballester, C. Rapisarda, S. Ferroni, and A. Ferrer-Montiel. 2005. Molecular compatibility of the channel gate and the N terminus of S5 segment for voltage-gated channel activity. *J. Biol. Chem.* 280:18253–18264. doi:10.1074/jbc.M413389200

Carter, R.N., G. Tolhurst, G. Walmsley, M. Vizuete-Forster, N. Miller, and M.P. Mahaut-Smith. 2006. Molecular and electrophysiological characterization of transient receptor potential ion channels in the primary murine megakaryocyte. *J. Physiol.* 576:151–162. doi:10.1113/jphysiol.2006.113886

Chen, J., J.S. Mitcheson, M. Tristani-Firouzi, M. Lin, and M.C. Sanguinetti. 2001. The S4-S5 linker couples voltage sensing and activation of pacemaker channels. *Proc. Natl. Acad. Sci. USA.* 98:11277–11282. doi:10.1073/pnas.201250598

Chen, X.-H., and R.W. Tsien. 1997. Aspartate substitutions establish the concerted action of P-region glutamates in repeats I and III in forming the protonation site of L-type Ca2+ channels. *J. Biol. Chem.* 272:30002–30008. doi:10.1074/jbc.272.48.30002

Choe, S. 2002. Potassium channel structures. *Nat. Rev. Neurosci.* 3:115–121. doi:10.1038/nrn727

Chubanov, V., K.P. Schlingmann, J. Wäring, J. Heinzinger, S. Kaske, S. Waldegger, M. Mederos y Schnitzler, and T. Gudermann. 2007. Hypomagnesemia with secondary hypocalcemia due to a missense mutation in the putative pore-forming region of TRPM6. *J. Biol. Chem.* 282:7656–7667. doi:10.1074/jbc.M611117200

Clapham, D.E. 2003. TRP channels as cellular sensors. *Nature.* 426:517–524. doi:10.1038/nature02196

Cohen, A., Y. Ben-Abu, S. Hen, and N. Zilberberg. 2008. A novel mechanism for human K2P2.1 channel gating. Facilitation of C-type gating by protonation of extracellular histidine residues. *J. Biol. Chem.* 283:19448–19455. doi:10.1074/jbc.M801273200

Csanády, L., and B. Törocsik. 2009. Four Ca^{2+} ions activate TRPM2 channels by binding in deep crevices near the pore but intracellularly of the gate. *J. Gen. Physiol.* 133:189–203. doi:10.1085/jgp.200810109

Du, J., J. Xie, and L. Yue. 2009. Intracellular calcium activates TRPM2 and its alternative spliced isoforms. *Proc. Natl. Acad. Sci. USA.* 106:7239–7244. doi:10.1073/pnas.0811725106

Fonfria, E., I.C.B. Marshall, I. Boyfield, S.D. Skaper, J.P. Hughes, D.E. Owen, W. Zhang, B.A. Miller, C.D. Benham, and S. McNulty. 2005. Amyloid β-peptide(1-42) and hydrogen peroxide-induced toxicity are mediated by TRPM2 in rat primary striatal cultures. *J. Neurochem.* 95:715–723. doi:10.1111/j.1471-4159.2005.03396.x

Gordon, S.E., J.C. Oakley, M.D. Varnum, and W.N. Zagotta. 1996. Altered ligand specificity by protonation in the ligand binding domain of cyclic nucleotide-gated channels. *Biochemistry.* 35:3994–4001. doi:10.1021/bi952607b

Hara, Y., M. Wakamori, M. Ishii, E. Maeno, M. Nishida, T. Yoshida, H. Yamada, S. Shimizu, E. Mori, J. Kudoh, et al. 2002. LTRPC2 Ca2+-permeable channel activated by changes in redox status confers susceptibility to cell death. *Mol. Cell.* 9:163–173. doi:10.1016/S1097-2765(01)00438-5

Hecquet, C.M., G.U. Ahmmed, S.M. Vogel, and A.B. Malik. 2008. Role of TRPM2 channel in mediating H2O2-induced Ca2+ entry and endothelial hyperpermeability. *Circ. Res.* 102:347–355. doi:10.1161/CIRCRESAHA.107.160176

Heiner, I., J. Eisfeld, C.R. Halaszovich, E. Wehage, E. Jüngling, C. Zitt, and A. Lückhoff. 2003a. Expression profile of the transient receptor potential (TRP) family in neutrophil granulocytes: evidence for currents through long TRP channel 2 induced by ADP-ribose and NAD. *Biochem. J.* 371:1045–1053. doi:10.1042/BJ20021975

Heiner, I., J. Eisfeld, and A. Lückhoff. 2003b. Role and regulation of TRP channels in neutrophil granulocytes. *Cell Calcium.* 33:533–540. doi:10.1016/S0143-4160(03)00058-7

Heiner, I., N. Radukina, J. Eisfeld, F. Kühn, and A. Lückhoff. 2005. Regulation of TRPM2 channels in neutrophil granulocytes by ADP-ribose: a promising pharmacological target. *Naunyn Schmiedebergs Arch. Pharmacol.* 371:325–333. doi:10.1007/s00210-005-1033-y

Heiner, I., J. Eisfeld, M. Warnstedt, N. Radukina, E. Jüngling, and A. Lückhoff. 2006. Endogenous ADP-ribose enables calcium-regulated cation currents through TRPM2 channels in neutrophil granulocytes. *Biochem. J.* 398:225–232. doi:10.1042/BJ20060183

Herson, P.S., and M.L. Ashford. 1997. Activation of a novel non-selective cation channel by alloxan and H2O2 in the rat insulin-secreting cell line CRI-G1. *J. Physiol.* 501:59–66. doi:10.1111/j.1469-7793.1997.059bo.x

Herson, P.S., K.A. Dulock, and M.L. Ashford. 1997. Characterization of a nicotinamide-adenine dinucleotide-dependent cation channel in the CRI-G1 rat insulinoma cell line. *J. Physiol.* 505:65–76. doi:10.1111/j.1469-7793.1997.065bc.x

Hill, K., N.J. Tigue, R.E. Kelsell, C.D. Benham, S. McNulty, M. Schaefer, and A.D. Randall. 2006. Characterisation of recombinant rat TRPM2 and a TRPM2-like conductance in cultured rat striatal neurones. *Neuropharmacology.* 50:89–97. doi:10.1016/j.neuropharm.2005.08.021

Jiang, J., M. Li, and L. Yue. 2005. Potentiation of TRPM7 inward currents by protons. *J. Gen. Physiol.* 126:137–150. doi:10.1085/jgp.200409185

Jordt, S.E., M. Tominaga, and D. Julius. 2000. Acid potentiation of the capsaicin receptor determined by a key extracellular site. *Proc. Natl. Acad. Sci. USA.* 97:8134–8139. doi:10.1073/pnas.100129497

Kaneko, S., S. Kawakami, Y. Hara, M. Wakamori, E. Itoh, T. Minami, Y. Takada, T. Kume, H. Katsuki, Y. Mori, and A. Akaike. 2006. A critical role of TRPM2 in neuronal cell death by hydrogen peroxide. *J. Pharmacol. Sci.* 101:66–76. doi:10.1254/jphs.FP0060128

Khan, A., L. Romantseva, A. Lam, G. Lipkind, and H.A. Fozzard. 2002. Role of outer ring carboxylates of the rat skeletal muscle

sodium channel pore in proton block. *J. Physiol.* 543:71–84. doi:10.1113/jphysiol.2002.021014

Kolisek, M., A. Beck, A. Fleig, and R. Penner. 2005. Cyclic ADP-ribose and hydrogen peroxide synergize with ADP-ribose in the activation of TRPM2 channels. *Mol. Cell.* 18:61–69. doi:10.1016/j.molcel.2005.02.033

Kozak, J.A., M. Matsushita, A.C. Nairn, and M.D. Cahalan. 2005. Charge screening by internal pH and polyvalent cations as a mechanism for activation, inhibition, and rundown of TRPM7/MIC channels. *J. Gen. Physiol.* 126:499–514. doi:10.1085/jgp.200509324

Kraft, R., C. Grimm, K. Grosse, A. Hoffmann, S. Sauerbruch, H. Kettenmann, G. Schultz, and C. Harteneck. 2004. Hydrogen peroxide and ADP-ribose induce TRPM2-mediated calcium influx and cation currents in microglia. *Am. J. Physiol. Cell Physiol.* 286:C129–C137. doi:10.1152/ajpcell.00331.2003

Kühn, F.J., and A. Lückhoff. 2004. Sites of the NUDT9-H domain critical for ADP-ribose activation of the cation channel TRPM2. *J. Biol. Chem.* 279:46431–46437. doi:10.1074/jbc.M407263200

Li, M., J. Jiang, and L. Yue. 2006. Functional characterization of homo- and heteromeric channel kinases TRPM6 and TRPM7. *J. Gen. Physiol.* 127:525–537. doi:10.1085/jgp.200609502

Li, M., J. Du, J. Jiang, W. Ratzan, L.-T. Su, L.W. Runnels, and L. Yue. 2007. Molecular determinants of Mg2+ and Ca2+ permeability and pH sensitivity in TRPM6 and TRPM7. *J. Biol. Chem.* 282:25817–25830. doi:10.1074/jbc.M608972200

Liu, D., Z. Zhang, and E.R. Liman. 2005. Extracellular acid block and acid-enhanced inactivation of the Ca2+-activated cation channel TRPM5 involve residues in the S3-S4 and S5-S6 extracellular domains. *J. Biol. Chem.* 280:20691–20699. doi:10.1074/jbc.M414072200

McHugh, D., R. Flemming, S.-Z. Xu, A.-L. Perraud, and D.J. Beech. 2003. Critical intracellular Ca2+ dependence of transient receptor potential melastatin 2 (TRPM2) cation channel activation. *J. Biol. Chem.* 278:11002–11006. doi:10.1074/jbc.M210810200

Middleton, R.E., D.J. Pheasant, and C. Miller. 1996. Homodimeric architecture of a ClC-type chloride ion channel. *Nature.* 383:337–340. doi:10.1038/383337a0

Montell, C. 2005. The TRP superfamily of cation channels. *Sci. STKE.* 2005:re3. doi:10.1126/stke.2722005re3

Nagamine, K., J. Kudoh, S. Minoshima, K. Kawasaki, S. Asakawa, F. Ito, and N. Shimizu. 1998. Molecular cloning of a novel putative Ca2+ channel protein (TRPC7) highly expressed in brain. *Genomics.* 54:124–131. doi:10.1006/geno.1998.5551

Naziroglu, M., and A. Luckhoff. 2008. A calcium influx pathway regulated separately by oxidative stress and ADP-ribose in TRPM2 channels: single channel events. *Neurochem. Res.* 33:1256–1262.

Nilius, B. 2007. TRP channels in disease. *Biochim. Biophys. Acta.* 1772:805–812.

Nimigean, C.M., J.S. Chappie, and C. Miller. 2003. Electrostatic tuning of ion conductance in potassium channels. *Biochemistry.* 42:9263–9268. doi:10.1021/bi0348720

Numata, T., and Y. Okada. 2008. Proton conductivity through the human TRPM7 channel and its molecular determinants. *J. Biol. Chem.* 283:15097–15103. doi:10.1074/jbc.M709261200

Perraud, A.L., A. Fleig, C.A. Dunn, L.A. Bagley, P. Launay, C. Schmitz, A.J. Stokes, Q. Zhu, M.J. Bessman, R. Penner, et al. 2001. ADP-ribose gating of the calcium-permeable LTRPC2 channel revealed by Nudix motif homology. *Nature.* 411:595–599. doi:10.1038/35079100

Perraud, A.L., C.L. Takanishi, B. Shen, S. Kang, M.K. Smith, C. Schmitz, H.M. Knowles, D. Ferraris, W. Li, J. Zhang, et al. 2005. Accumulation of free ADP-ribose from mitochondria mediates oxidative stress-induced gating of TRPM2 cation channels. *J. Biol. Chem.* 280:6138–6148. doi:10.1074/jbc.M411446200

Rajdev, S., and I.J. Reynolds. 1995. Calcium influx but not pH or ATP level mediates glutamate-induced changes in intracellular magnesium in cortical neurons. *J. Neurophysiol.* 74:942–949.

Runnels, L.W., L. Yue, and D.E. Clapham. 2002. The TRPM7 channel is inactivated by PIP(2) hydrolysis. *Nat. Cell Biol.* 4:329–336.

Ryu, S., B. Liu, and F. Qin. 2003. Low pH potentiates both capsaicin binding and channel gating of VR1 receptors. *J. Gen. Physiol.* 122:45–61. doi:10.1085/jgp.200308847

Sano, Y., K. Inamura, A. Miyake, S. Mochizuki, H. Yokoi, H. Matsushime, and K. Furuichi. 2001. Immunocyte Ca2+ influx system mediated by LTRPC2. *Science.* 293:1327–1330. doi:10.1126/science.1062473

Semtner, M., M. Schaefer, O. Pinkenburg, and T.D. Plant. 2007. Potentiation of TRPC5 by protons. *J. Biol. Chem.* 282:33868–33878. doi:10.1074/jbc.M702577200

Siesjö, B.K. 1988. Acidosis and ischemic brain damage. *Neurochem. Pathol.* 9:31–88.

Starkus, J., A. Beck, A. Fleig, and R. Penner. 2007. Regulation of TRPM2 by extra- and intracellular calcium. *J. Gen. Physiol.* 130:427–440. doi:10.1085/jgp.200709836

Togashi, K., Y. Hara, T. Tominaga, T. Higashi, Y. Konishi, Y. Mori, and M. Tominaga. 2006. TRPM2 activation by cyclic ADP-ribose at body temperature is involved in insulin secretion. *EMBO J.* 25:1804–1815. doi:10.1038/sj.emboj.7601083

Venkatachalam, K., and C. Montell. 2007. TRP channels. *Annu. Rev. Biochem.* 76:387–417. doi:10.1146/annurev.biochem.75.103004.142819

Voets, T., G. Owsianik, A. Janssens, K. Talavera, and B. Nilius. 2007. TRPM8 voltage sensor mutants reveal a mechanism for integrating thermal and chemical stimuli. *Nat. Chem. Biol.* 3:174–182. doi:10.1038/nchembio862

Wehage, E., J. Eisfeld, I. Heiner, E. Jüngling, C. Zitt, and A. Lückhoff. 2002. Activation of the cation channel long transient receptor potential channel 2 (LTRPC2) by hydrogen peroxide. A splice variant reveals a mode of activation independent of ADP-ribose. *J. Biol. Chem.* 277:23150–23156. doi:10.1074/jbc.M112096200

Xia, R., Z.Z. Mei, H.J. Mao, W. Yang, L. Dong, H. Bradley, D.J. Beech, and L.H. Jiang. 2008. Identification of pore residues engaged in determining divalent cationic permeation in transient receptor potential melastatin subtype channel 2. *J. Biol. Chem.* 283:27426–27432. doi:10.1074/jbc.M801049200

Yamamoto, S., S. Shimizu, S. Kiyonaka, N. Takahashi, T. Wajima, Y. Hara, T. Negoro, T. Hiroi, Y. Kiuchi, T. Okada, et al. 2008. TRPM2-mediated Ca(2+) influx induces chemokine production in monocytes that aggravates inflammatory neutrophil infiltration. *Nat. Med.* 14:738–747.

Yeh, B.-I., T.-J. Sun, J.Z. Lee, H.-H. Chen, and C.-L. Huang. 2003. Mechanism and molecular determinant for regulation of rabbit transient receptor potential type 5 (TRPV5) channel by extracellular pH. *J. Biol. Chem.* 278:51044–51052. doi:10.1074/jbc.M306326200

Yue, L., J.L. Feng, Z. Wang, and S. Nattel. 2000. Effects of ambasilide, quinidine, flecainide and verapamil on ultra-rapid delayed rectifier potassium currents in canine atrial myocytes. *Cardiovasc. Res.* 46:151–161. doi:10.1016/S0008-6363(99)00430-7

Yue, L., B. Navarro, D. Ren, A. Ramos, and D. Clapham. 2002. The cation selectivity filter of the bacterial sodium channel, NaChBac. *J. Gen. Physiol.* 120:845–853. doi:10.1085/jgp.20028699

Zhang, W., I. Hirschler-Laszkiewicz, Q. Tong, K. Conrad, S.C. Sun, L. Penn, D.L. Barber, R. Stahl, D.J. Carey, J.Y. Cheung, and B.A. Miller. 2006. TRPM2 is an ion channel that modulates hematopoietic cell death through activation of caspases and PARP cleavage. *Am. J. Physiol. Cell Physiol.* 290:C1146–C1159. doi:10.1152/ajpcell.00205.2005Supplemental material